GS-3 Geological investigations of the Cat Creek area in the Neoarchean Bird River greenstone belt, southeastern Manitoba (part of NTS 52L12): new insights into PGE-Ni-Cu-Cr mineralization

by X.M. Yang, H.P. Gilbert and M.G. Houlé[1]

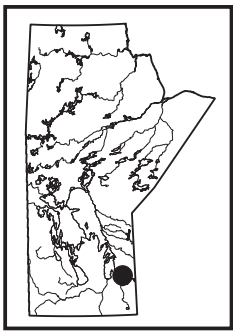

Yang, X.M., Gilbert, H.P. and Houlé, M.G. 2012: Geological investigations of the Cat Creek area in the Neoarchean Bird River greenstone belt, southeastern Manitoba (part of NTS 52L12): new insights into PGE-Ni-Cu-Cr mineralization; *in* Report of Activities 2012, Manitoba Innovation, Energy and Mines, Manitoba Geological Survey, p. 32–53.

Summary

The Cat Creek area in the northern arm of the Bird River greenstone belt is situated approximately 145 km northeast of Winnipeg in southeastern Manitoba. The study area is underlain by a suite of typical greenstone assemblages within a continental-margin setting adjacent to the Mesoarchean Maskwa Lake Batholith. The rock assemblages consist of a tonalite-trondhjemite-granodiorite suite; supracrustal rocks that include mafic to felsic volcanic and synvolcanic intrusive rocks, and epiclastic and minor volcaniclastic rocks; the Mayville mafic–ultramafic layered intrusion; and late peraluminous granitoid rocks and related pegmatites. The Mayville intrusion consists of an east-trending lopolith approximately 10.5 km in length and up to 1.5 km in width. The intrusion is emplaced in a mid-ocean-ridge basalt (MORB) sequence to the south and west and is in structural contact with granitoid rocks to the east. To the north, the Mayville intrusion is emplaced in metasedimentary and intercalated volcaniclastic rocks, and is locally structurally juxtaposed against granitoid rocks. Although the Mayville intrusion has recently been the focus of ongoing mineral exploration because it hosts a significant amount of platinum group element (PGE)–Ni–Cu–Cr mineralization, some key metallogenic questions remain to be answered.

This report presents the preliminary results of geological mapping conducted at a scale of 1:12 500 by the Manitoba Geological Survey in 2012, together with new petrological, lithogeochemical and geochronological data acquired within the last year. Twelve map units have been identified in the Cat Creek area. The mapping and geochemical study suggest that the MORB-type basalts and related intrusive rocks, as well as the Mayville intrusion, may have been emplaced in an extensional back-arc environment characterized by a relatively thin crust (~21 km) and a continental-margin setting. The present geological map data indicate that the Neoarchean Mayville intrusion (U-Pb zircon age of 2743 Ma) consists dominantly of anorthositic gabbro, gabbroic anorthosite and anorthosite, with subordinate melagabbro and pyroxenite at the base and gabbro at the top. This intrusion is similar to Archean anorthosite complexes elsewhere, and can be subdivided into a lower heterolithic breccia zone and an upper anorthosite to leucogabbro zone. The geochemical signature of the Mayville intrusion suggests the parental magma(s) was an alumina-enriched tholeiitic type that may have been derived from a high degree of partial melting of the subcontinental lithospheric mantle; it may have experienced assimilation and fractional crystallization during its emplacement within the supracrustal rock succession. An early sulphide saturation event triggered by crustal contamination and/or introduced external sulphur is likely to have generated magmatic sulphide Ni-Cu-PGE mineralization at the base of the intrusion. The injection of a new batch(s) of a mafic–ultramafic melt may have resulted in PGE and chromite mineralization at transitional zones between various phases within the intrusion. In addition, calcic anorthosite in the Mayville intrusion may represent a potential source for the manufacture of aluminum-bearing chemicals.

Introduction

In 2011, the Manitoba Geological Survey (MGS) initiated a multiyear bedrock geological mapping project focusing on the Cat Creek and Cat Lake–Euclid Lake areas in the northern arm of the Bird River greenstone belt (BRGB), within the western Superior Province. This project is conducted in collaboration with the Geological Survey of Canada (GSC) through the Targeted Geoscience Initiative Phase IV (TGI-4) program, and supported by mining companies including Mustang Minerals Corp. The main objectives of the project are to 1) update the regional geological mapping in the Cat Creek and Cat Lake–Euclid Lake areas, 2) address the geological evolution and the geodynamic environment, and 3) assess the metallogeny of magmatic sulphide Ni-Cu-PGE-Cr mineralization within the BRGB.

This report presents the preliminary results of geological mapping at a scale of 1:12 500 conducted by the MGS this past summer, together with new petrological, lithogeochemical and geochronological data acquired over the last year. Furthermore, a more detailed and modern geological map covering the Cat Lake–Euclid Lake areas, including a detailed geological map of the Cat Creek area, is designed to aid mineral exploration, in particular for magmatic Ni-Cu-PGE-Cr mineralization.

[1] Geological Survey of Canada, 490 rue de la Couronne, Québec, Quebec G1K 9A9

Previous work

The BRGB has long been the subject of geological investigations, primarily because it contains magmatic Ni-Cu-PGE-Cr minerals, a world-class Cs–Ta–Nb–Li–rare earth element (REE) deposit at the TANCO mine, and numerous other mineral occurrences, such as Au and Cu-Zn (Springer, 1949, 1950; Trueman and Macek, 1971; Trueman, 1980; Scoates, 1983; Macek, 1985a, b; Theyer, 1986, 2003; Scoates et al., 1989; Peck et al., 1999, 2000, 2002; Hulbert and Scoates, 2000; Gilbert, 2006, 2007; Kremer and Lin, 2006; Gilbert et al., 2008; Mealin, 2008; Duguet et al., 2009; Good et al., 2009; Kremer, 2010; Stott et al., 2010). Its tectonic location between two continental cratonic blocks, the English River and Winnipeg River subprovinces (Figure GS-3-1), guides the general understanding of the BRGB, corroborated by systematic geological and multidisciplinary investigations (e.g., Beaumont-Smith et al., 2003; Percival et al., 2006a, b; Anderson, 2007, 2008; Percival, 2007; Corkery et al., 2010), as well as larger scale studies on geodynamic processes involving the assembly of different terranes within the Archean craton (e.g., Hoffman, 1988; Böhm et al., 2000; Burke, 2011).

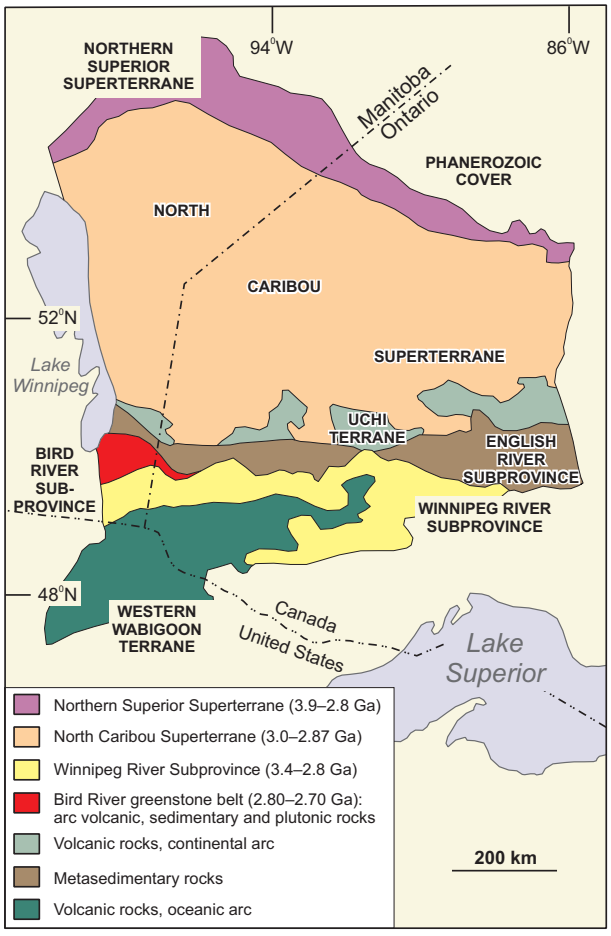

Figure GS-3-1: *Simplified geology of the western Superior Province, showing the location of the Neoarchean Bird River greenstone belt (BRGB; after Gilbert, 2007), southeastern Manitoba.*

Regional geological mapping at a scale of 1 inch to 1 mile (1:63 360) in the area between Maskwa Lake and Cat Lake, as well as in the Bird River area to the south, was carried out by Springer (1949, 1950). He concluded that the dominant structure in the region is anticlinal, with the Bird River Sill (BRS; Figure GS-3-2) in the south limb dipping steeply to the south, and the north limb (including the Mayville intrusion) being partly overturned and also dipping to the south. Springer (1949, 1950) implied that the configuration of the mafic–ultramafic BRS, the Mayville intrusion and analogous rocks at Euclid Lake reflect the closure of an east-plunging anticlinal fold. This interpretation was supported by Trueman and Macek (1971), Trueman (1980), Černý et al. (1981) and Macek (1985a, b). The regional bedrock geology, including the BRGB, was compiled by the MGS at a scale of 1:250 000 (Manitoba Energy and Mines, 1987), as well as by subsequent collaborative mapping projects involving the MGS, GSC and Ontario Geological Survey (Bailes et al., 2003; Lemkow et al., 2006).

Macek (1985b) published a preliminary 1:10 000 scale geological map of the western part of the Mayville intrusion and surrounding rocks, and tentatively suggested that the intrusion is part of the BRB. Subsequently, detailed geological mapping was carried out by various mineral-exploration companies (e.g., Exploratus Ltd., Falconbridge Ltd., Tantalum Mining Corporation of Canada Ltd.) on their respective properties. Most recently, Mustang Minerals Corp. completed 1:1 000 scale geological mapping of the western part of the Mayville intrusion, where diamond-drilling targeted rocks hosting PGE-Cu-Ni-Cr mineralization (Mustang Minerals Corp., 2011; Galeschuk, pers. comm., 2012).

In 2005, MGS initiated a four-year mapping project focusing on the main, southern part of the BRGB, in collaboration with several universities and mineral-exploration companies (Gilbert, 2008; Gilbert and Kremer, 2008; Gilbert et al., 2008). The northern limb of the BRGB (Cat Creek–Euclid Lake area; Figure GS-3-2) has, however, received less attention.

Regional geology

The Neoarchean BRGB is situated between the English River and Winnipeg River subprovinces of the western Superior Province (Figure GS-3-1; Peck et al., 2002; Gilbert et al., 2008). It is part of an approximately 150 km long, east-trending supracrustal belt that extends from Lac du Bonnet in the west to Separation Lake (Ontario) in the east, where it is termed the 'Separation Lake greenstone belt' (Percival et al., 2006a, b). Regional aeromagnetic data and Nd-isotope evidence suggest that the BRGB extends westward beneath the Paleozoic sedimentary cover for at least 300 km (McGregor, 1986; Stevenson et al., 2000; Percival et al., 2006b). Investigations of the complex history of deformation, tectonism,

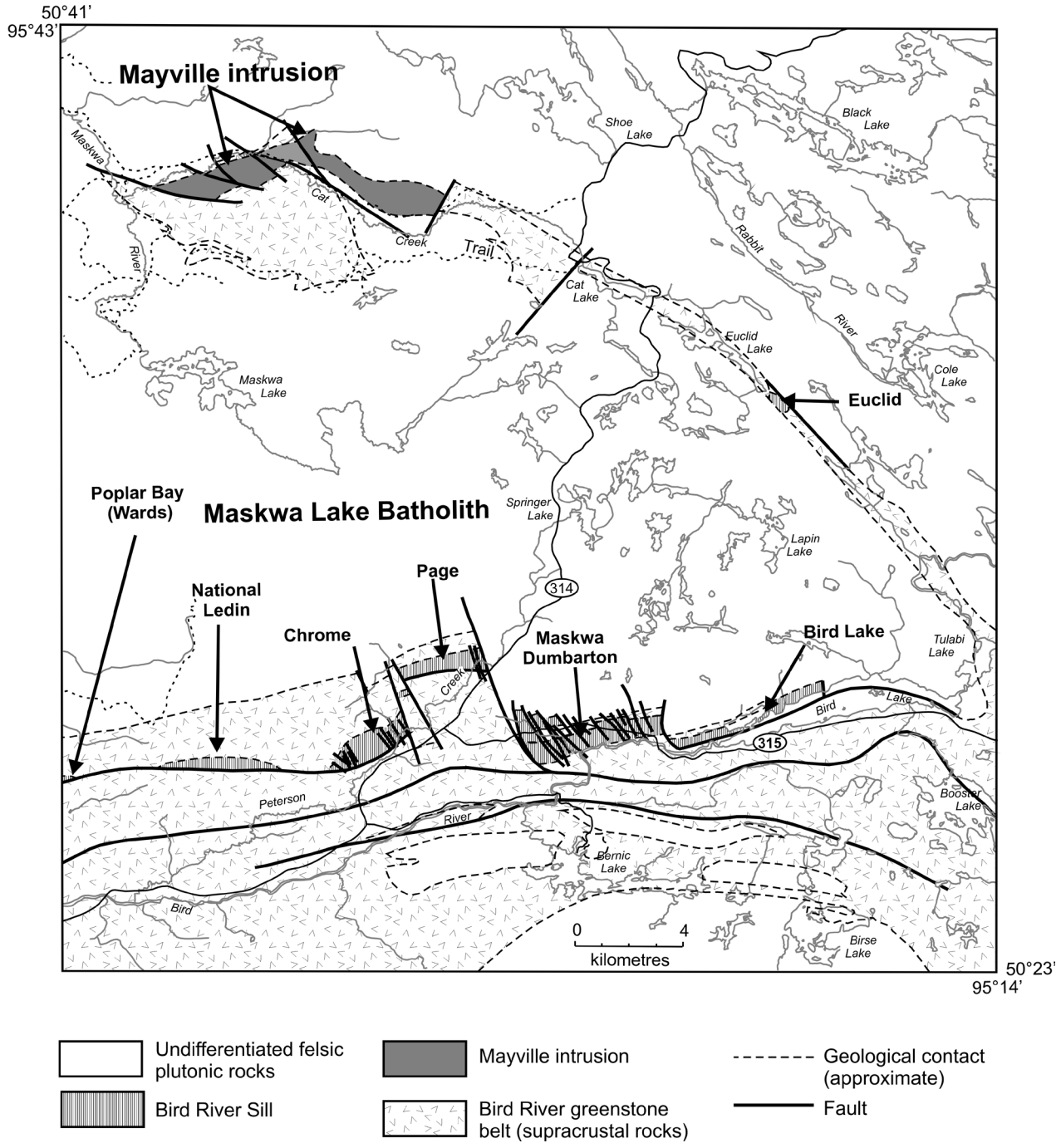

Figure GS-3-2: *Simplified geology of the Neoarchean Bird River greenstone belt, showing the location of the Mayville mafic–ultramafic intrusion and the Bird River Sill (after Peck et al., 2002) in southeastern Manitoba.*

metamorphism, magmatism and associated mineralization in the southern part of the BRGB (Percival, 2007; Duguet et al., 2009) have shown it to be in a key position for studies of crustal tectonic processes and the geodynamics of ancient cratons, with reference to modern concepts of plate tectonics (e.g., Hoffman, 1988; Burke, 2011). These studies have also indicated that the greenstone belt is a prospective area for base metals (Ni, Cu, Cr), precious metals (PGEs, Au), rare metals (Ta, Cs, Nb, Li) and REEs.

The emplacement of both the BRS and the Mayville mafic–ultramafic intrusion (see below), which host magmatic Ni-Cu-PGE-Cr mineralization, appears to have taken place at some stage(s) during ca. 2.80–2.70 Ga continental-arc magmatism and orogenic sedimentation (Percival et al., 2006a, b; Gilbert et al., 2008). However, the geodynamic setting into which these mafic–ultramafic intrusion(s) were emplaced has long been debated and is the focus of the current multidisciplinary research.

Geology of the Cat Creek area

The Cat Creek area is located in the northern limb of the BRGB (Figure GS-3-2), which is underlain by a suite of typical greenstone assemblages. These greenstone assemblages, which occur in a continental-margin setting adjacent to the Mesoarchean Maskwa Lake Batholith, consist of a tonalite-trondhjemite-granodiorite (TTG) suite; supracrustal rocks that include mafic to felsic volcanic and related intrusive rocks, and epiclastic and minor volcaniclastic rocks; mafic–ultramafic layered intrusion(s); and late peraluminous granitoid rocks and related pegmatites. The Mayville mafic–ultramafic intrusion consists of an east-trending lopolith approximately 10.5 km in length and up to 1.5 km in width. The intrusion is emplaced in a mid-ocean-ridge basalt (MORB) sequence to the south and west, and is in structural contact with granitoid rocks to the east. To the north, the Mayville intrusion is emplaced in metasedimentary and intercalated volcaniclastic rocks, and is locally structurally juxtaposed against granitoid rocks.

Twelve map units have been identified in the Cat Creek area on the basis of systematic geological mapping conducted at a scale of 1:12 500 by the MGS this past summer. These are, from oldest to youngest (Yang, 2012), 1) Maskwa Lake Batholith granitoid rocks; 2) MORB-type basaltic and synvolcanic intrusive rocks; 3) metasedimentary rocks and thin intercalated volcaniclastic rocks; 4) to 10) mafic–ultramafic rocks of the Mayville intrusion, consisting of basal melagabbro and pyroxenite (unit 4), heterolithic breccias (unit 5), gabbroic anorthosite to anorthosite (unit 6), leucogabbro (unit 7), gabbro (unit 8), diabasic to gabbroic rocks (unit 9) and quartz diorite to granodiorite (unit 10); 11) granitoid rocks (TTG; garnet-muscovite–bearing granite); and 12) pegmatites. Representative whole-rock geochemistry and petrographic analysis from each map unit are in progress.

Maskwa Lake Batholith granitoid rocks (unit 1)

The Maskwa Lake Batholith is a multiphase felsic intrusion composed of granodioritic and dioritic phases. Coarse-grained, locally porphyritic, pink granodiorite of the Maskwa Lake Batholith in the southern part of the map area (Yang, 2012) is in contact with massive and pillowed basalt to the south (unit 2; see below), which is comparable to the northern MORB-type formation of Gilbert et al. (2008). The granitoid rocks are brecciated and fragmented by basalt (Figure GS-3-3a, b), indicating that basalt is younger than granodiorite. Uranium-lead zircon ages of the oldest known granitoid phase(s) in the Maskwa Lake Batholith range from 2852.8 ±1.1 Ma (Gilbert et al., 2008) to 2844 ±12 Ma (Wang, 1993). Relatively younger granitoid phases in the batholith include quartz diorite, tonalite and granodiorite to granite; these have been dated at 2725 ±6 Ma (Wang, 1993) and are therefore younger than the BRS (2744.7 ±5.2 Ma; Wang, 1993), as well as the northern MORB-type formation in which the sill is emplaced (Gilbert et al., 2008).

MORB-type basalt and synvolcanic intrusive rocks (unit 2)

Mid-ocean-ridge basalt–type basalt is intermittently exposed within the southern part of the Mayville intrusion. The massive to pillowed basalt flows contain or are cut by gabbroic dikes and sills, and are very fine grained to aphanitic; basalt is largely aphyric, but locally includes plagioclase porphyritic and megaphyric units (Figure GS-3-3c–e). A megacrystic gabbroic anorthosite to anorthosite sill is exposed west of the Donner Lake Road (Yang, 2012). Igneous layering, defined by grain-size variation, suggests the sill is north facing, consistent with north-facing pillowed flows in the same area (Macek, 1985a; Peck et al., 2002; Yang et al., 2011).

Unit 2 basalt is strongly foliated and metamorphosed to greenschist to lower amphibolite facies; it consists largely of very fine grained, elongate amphibole and plagioclase laths, typically aligned within foliation planes, with chlorite, epidote and albite. Disseminated magnetite is common, and pyrrhotite (±pyrite±chalcopyrite) occurs locally in the basalt (Figure GS-3-3f). Unit 2 basalt is geochemically and petrologically equivalent to the northern MORB-type formation of Gilbert et al. (2008).

Metasedimentary rocks and thin volcaniclastic rocks (unit 3)

Metasedimentary rocks and intercalated thin volcaniclastic sandstone beds outcrop mainly in the northern and western parts of the map area (Yang, 2012), close to the margin of the Mayville mafic–ultramafic intrusion. The main rock types in unit 3 are well-layered (1–10 cm) greywacke and siltstone (Figure GS-3-4a), fine- to medium-grained sandstone and laminated gneiss containing garnet porphyroblasts (Figure GS-3-4b, c, e, f). Matrix-supported polymictic conglomerate with felsic volcanic and granitoid clasts occurs locally at the base of unit 3 rocks. A very coarse fragmental rock, with clasts that are ovoid to amoeboid, rimmed and unsorted to randomly distributed, constitutes either a debris flow or a volcanic breccia (Figure GS-3-4d). Volcaniclastic sandstone with intermediate volcanic clasts occurs as a thin bed within unit 3 rocks. Alternating biotite-amphibole-garnet and feldspar-quartz layers within a lithic, fragment-rich greywacke/sandstone bed suggest metamorphic differentiation and an amphibolite-facies grade of metamorphism. Late granitoid and pegmatite dikes and veins are emplaced within this unit.

Contact relationships between unit 3 and the Mayville intrusion were not observed, but one exposure of fine-grained greywacke-siltstone near the margin of the intrusion north of Cat Creek contains prominent amphibole and garnet porphyroblasts that are interpreted to be

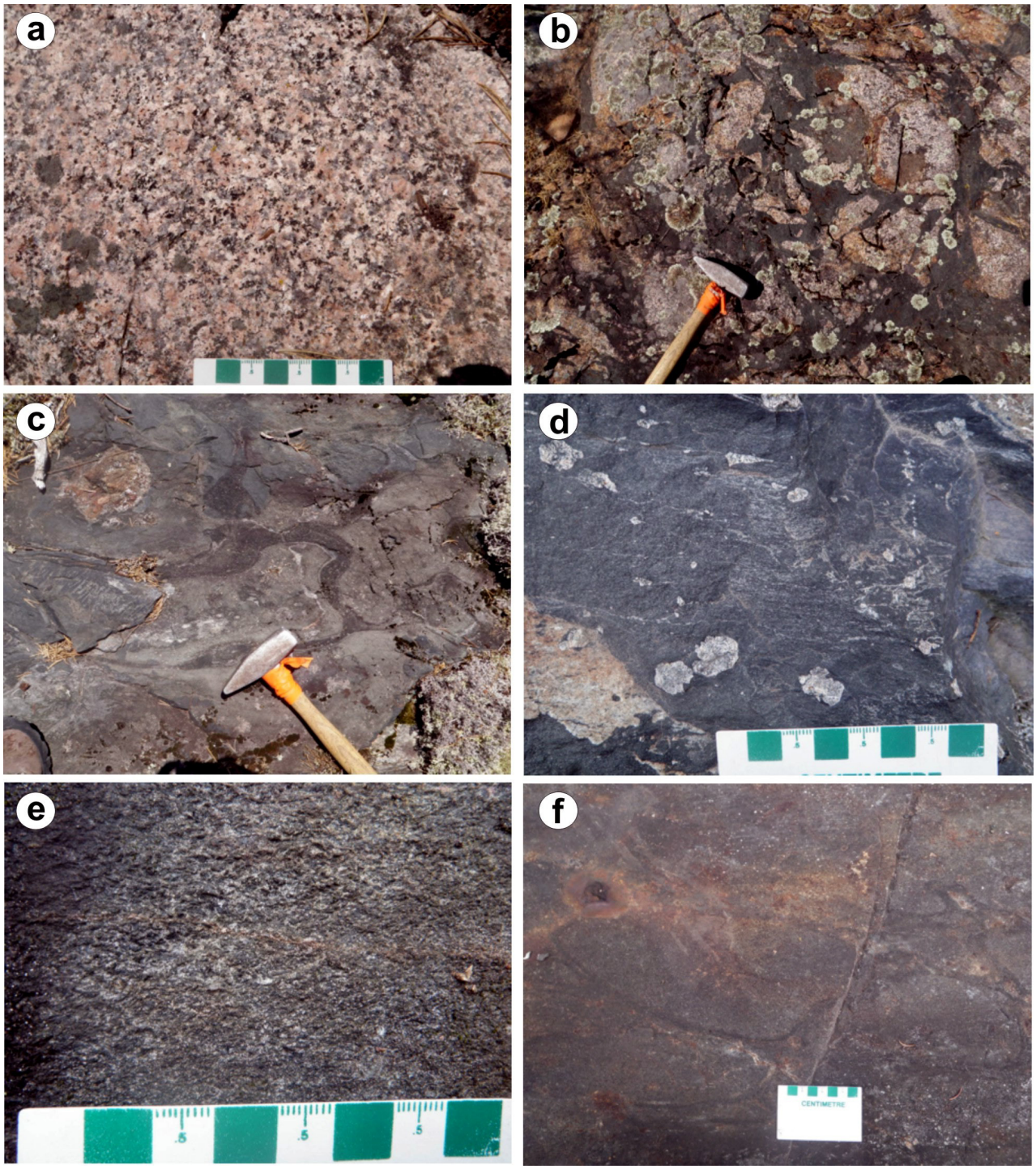

Figure GS-3-3: *Field photographs of map units 1 and 2, showing lithological characteristics and/or field relationships, Cat Creek area, southeastern Manitoba:* ***a****) medium- to coarse-grained, massive pink granodiorite with subhedral K-feldspar phenocrysts, Maskwa Lake Batholith (unit 1; UTM Zone 15N, 315347E, 5608476N, NAD83);* ***b****) Maskwa Lake Batholith granodiorite breccia (unit 1) at the contact zone with basalt; fragments are cemented by very fine grained basalt (unit 2), suggesting that this phase of the Maskwa Lake Batholith is older than the basalt (UTM 315337E, 5608472N);* ***c****) pillowed basalt flow (unit 2) with granitoid xenolith similar to the Maskwa Lake granodiorite (UTM 315261E, 5609647N);* ***d****) plagioclase-phyric basalt (unit 2) cut by a late fine-grained granitoid dike (lower left corner; UTM 314038E, 5611851N);* ***e****) fine-grained massive gabbro (unit 2a) as a dike in MORB-type basalt (UTM 313963E, 5611679N);* ***f****) pillowed foliated basalt (unit 2) with iron-oxide–stained surface and disseminated pyrrhotite (UTM 313836E, 5611527N).*

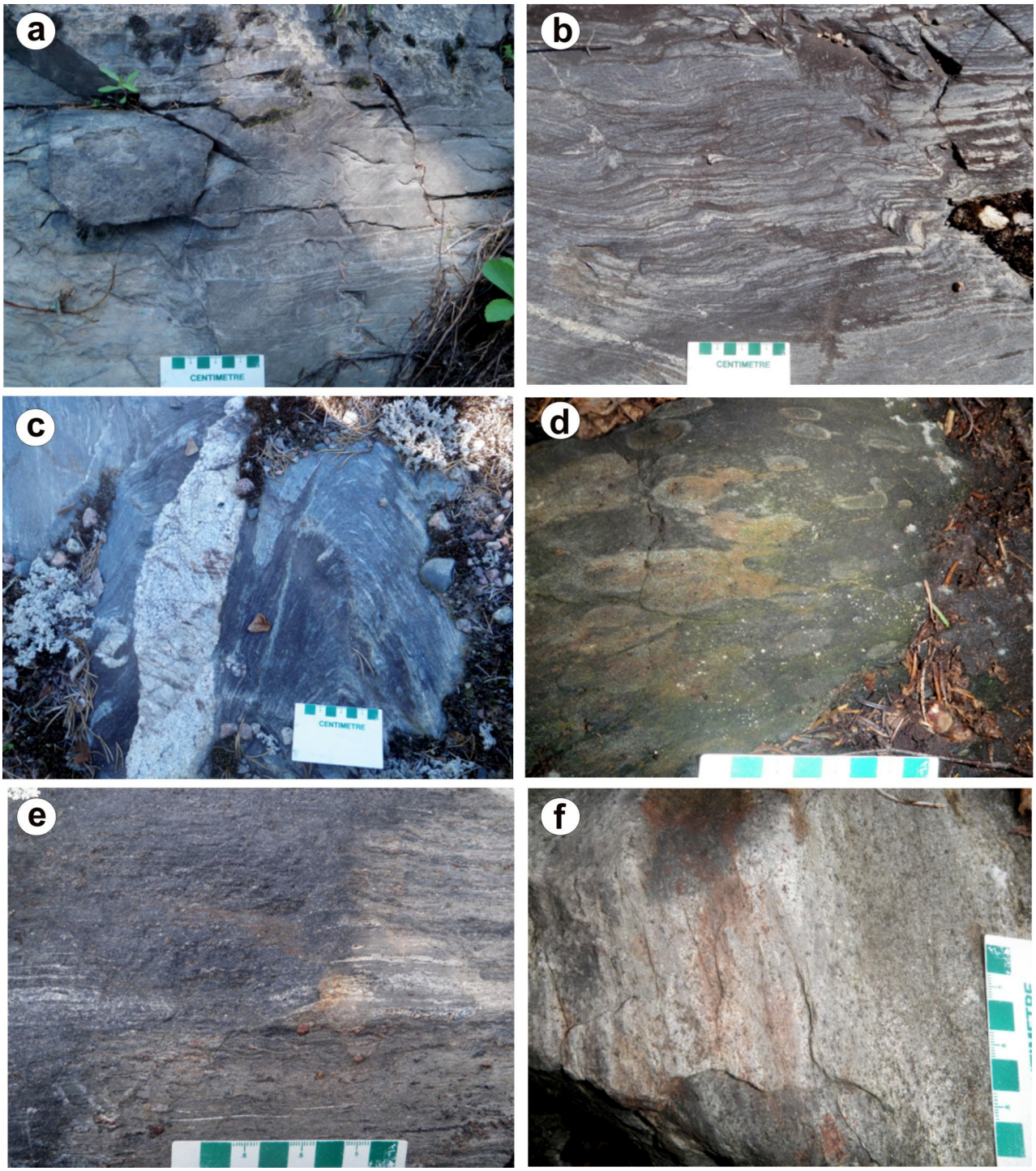

Figure GS-3-4: *Field photographs of map unit 3, exhibiting lithological characteristics and/or field relationships, Cat Creek area, southeastern Manitoba:* ***a****) well-bedded greywacke (UTM Zone 15N, 315176E, 5613405N, NAD83);* ***b****) folded gneiss containing felsic veins that are both parallel and discordant to the foliation plane (UTM 312461E, 5613304N);* ***c****) folded gneiss, cut by a late granite dike (UTM 312461E, 5613304N);* ***d****) volcanic breccia or debris flow (UTM 315939E, 5613300N);* ***e****) laminated garnet-porphyroblastic greywacke (UTM 315401E, 5613350N);* ***f****) well-bedded siltstone and greywacke containing disseminated pyrite (UTM 315357E, 5613415N).*

the result of hornfels development (i.e., contact metamorphism) associated with the Mayville intrusion.

Mayville mafic–ultramafic intrusion (units 4 to 10)

The Mayville mafic–ultramafic intrusion is a Neoarchean layered intrusion (Macek, 1985a; Peck et al., 1999, 2002; Theyer, 2003; Yang et al., 2011) that consists dominantly of anorthositic gabbro[2], gabbroic anorthosite and anorthosite, with subordinate melagabbro and pyroxenite at the base and gabbro at the top. The Mayville intrusion is similar to Archean anorthosite complexes, and can generally be subdivided into a lower heterolithic breccia zone (HBX) and an upper anorthosite to leucogabbro zone (ALZ), as suggested by detailed trench mapping (Peck et al., 1999, 2002; Theyer, 2003). Seven mappable units are divided and described in the following subsections.

Basal mafic–ultramafic rocks (unit 4)

This map unit occurs at the base within the western portion of the Mayville intrusion, but is absent in the eastern portion where the southern contact of the intrusion is in fault contact with granodiorite to tonalite. The basal mafic–ultramafic unit consists mainly of fine- to medium-grained melagabbro, and medium- to coarse-grained, locally strongly foliated and magnetite-bearing chlorite-amphibole schist and hornblendite (both after pyroxenite; Figure GS-3-5a). This basal unit is estimated to be up to 100 m thick, although its southern extent is largely covered by swamps and/or thick marsh. Disrupted chromitite layers or bands are locally present in the upper part of the unit (Figure GS-3-5b), and disseminated chromite is evident in some places. Diamond-drilling intersected a chromitite zone, up to 5.9 m in width (PGE zone; drillhole MAY-11-07 of Mustang Minerals Corp.), the occurrence of which is supported by chromitite banding and disseminated chromite in pyroxenite reported by Hiebert (2003).

Magnetite stringers and thin layers are locally common and exhibit strong magnetic response (Figure GS-3-5c). Nonmagnetic chlorite-amphibole schist, however, is also evident in unit 4 (Figure GS-3-5d).

Disseminated, semimassive to massive sulphide minerals, consisting mainly of pyrrhotite, chalcopyrite and pentlandite, are commonly present in this unit, particularly at the bottom of the M2 deposit (Figure GS-3-5e), M2W zone, the Copper Contact zone and the Hititrite occurrence (Yang et al., 2011; Galeschuk, pers. comm., 2012).

Heterolithic breccias (unit 5)

Heterolithic breccias (HBX), or the heterolithic breccia zone described by Peck et al. (2002) and Mackie (2003), are composed of diverse rock types, including medium- to coarse-grained and megacrystic, variably textured melagabbro, gabbro and pyroxenite, as well as various associated pegmatitic or megacrystic leucogabbro and anorthosite phases that occur as irregular pods, patches, veins and layers ranging up to 100 m in thickness (Figure GS-3-5e). Basalt xenoliths from the country rocks occur in the lower part of the HBX, and irregular leucogabbro to anorthosite fragments (Figure GS-3-5f) are locally evident higher up in this unit. The most southerly (inferred basal) HBX appears to have been emplaced later than the upper leucogabbro and anorthosite units because the HBX contains leucogabbro and anorthosite fragments that appear to have been derived from the ALZ. The HBX is locally intruded by fine- to medium-grained quartz diorite to tonalite. These dikes locally contain rare sulphide disseminations. Sulphide minerals (mainly pyrrhotite with minor chalcopyrite±pyrite) occur sporadically in the HBX as disseminations, net-textured veins and/or locally massive sulphide bands. Massive chromitite bands and disrupted chromitite-pyroxenite layers are locally present in the middle to upper parts of the HBX (Peck et al., 2002; Hiebert, 2003).

The eastern part of the Mayville intrusion (i.e., east of the Donner Lake Road) lacks the HBX and, at the top, the gabbro (unit 8; see below).

Gabbroic anorthosite to anorthosite (unit 6)

Unit 6 comprises very coarse grained to megacrystic, locally glomeroporphyritic, gabbroic anorthosite to anorthosite. In the gabbroic anorthosite, calcic plagioclase occurs as equant, euhedral to subhedral crystals up to 10 cm in size, accounting for >80% of the rock, with minor interstitial amphibole after pyroxene (Figure GS-3-5g). If amphibole constitutes less than 10% of plagioclase-rich rock, it is termed anorthosite (Ashwal, 1993), which is mineralogically very similar to gabbroic anorthosite.

Unit 6 is a relatively thin (less than 50 m) but persistent member of the Mayville intrusion. Where megacrystic subrounded plagioclase occurs in the rock, it is called 'golf-ball' leucogabbro or anorthosite (Galeschuk, pers. comm., 2012). At one locality, gabbroic anorthosite is strongly sheared and displays only a few sporadic plagioclase megacryst relicts (Figure GS-3-5h). Sulphide minerals are rarely present in this unit.

Leucogabbro (unit 7)

Leucogabbro (Figure GS-3-6a) is the most abundant rock type within the Mayville intrusion. Igneous layering is present in various places in this unit, defined by

[2] The prefix 'meta-' for these rock types is omitted in this report for simplicity.

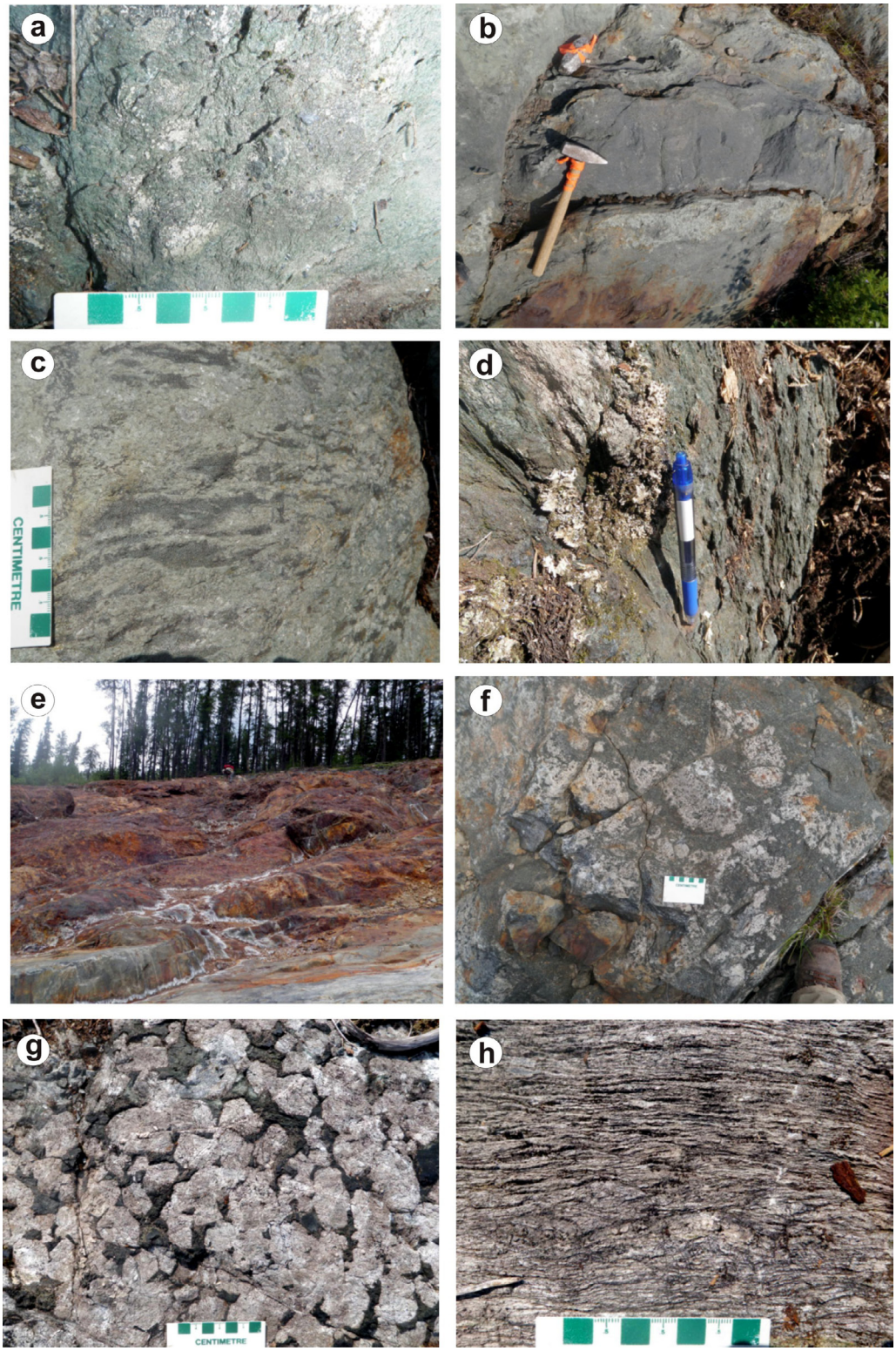

Figure GS-3-5: *Field photographs of the Mayville intrusion, showing lithological characteristics and/or field relationships, Cat Creek area, southeastern Manitoba:* ***a****) foliated chlorite-magnetite-amphibole schist (after pyroxenite) with strong magnetic property (unit 4; UTM Zone 15N, 313763E, 5612308N, NAD83);* ***b****) disrupted, ~40 cm thick chromitite band in pyroxenite (UTM 314616E, 5612596N);* ***c****) magnetite stringers in pyroxenite (UTM 314610E, 5612593N);* ***d****) sulphide-bearing chlorite-amphibole schist (after pyroxenite; unit 4) without notable magnetism (UTM 313108E, 56123391N);* ***e****) mineralized heterolithic breccia zone at the M2 deposit (unit 5; UTM 315410E, 5612608N);* ***f****) leucogabbro to anorthosite fragments and/or breccia cemented by melagabbro matrix in the heterolithic breccia zone (unit 5; UTM 5612630E, 315405N);* ***g****) megacrystic anorthosite (unit 6; UTM 319580E, 5611714N);* ***h****) sheared gabbroic anorthosite with mylonitic characteristics (unit 6; UTM 319438E, 5611789N).*

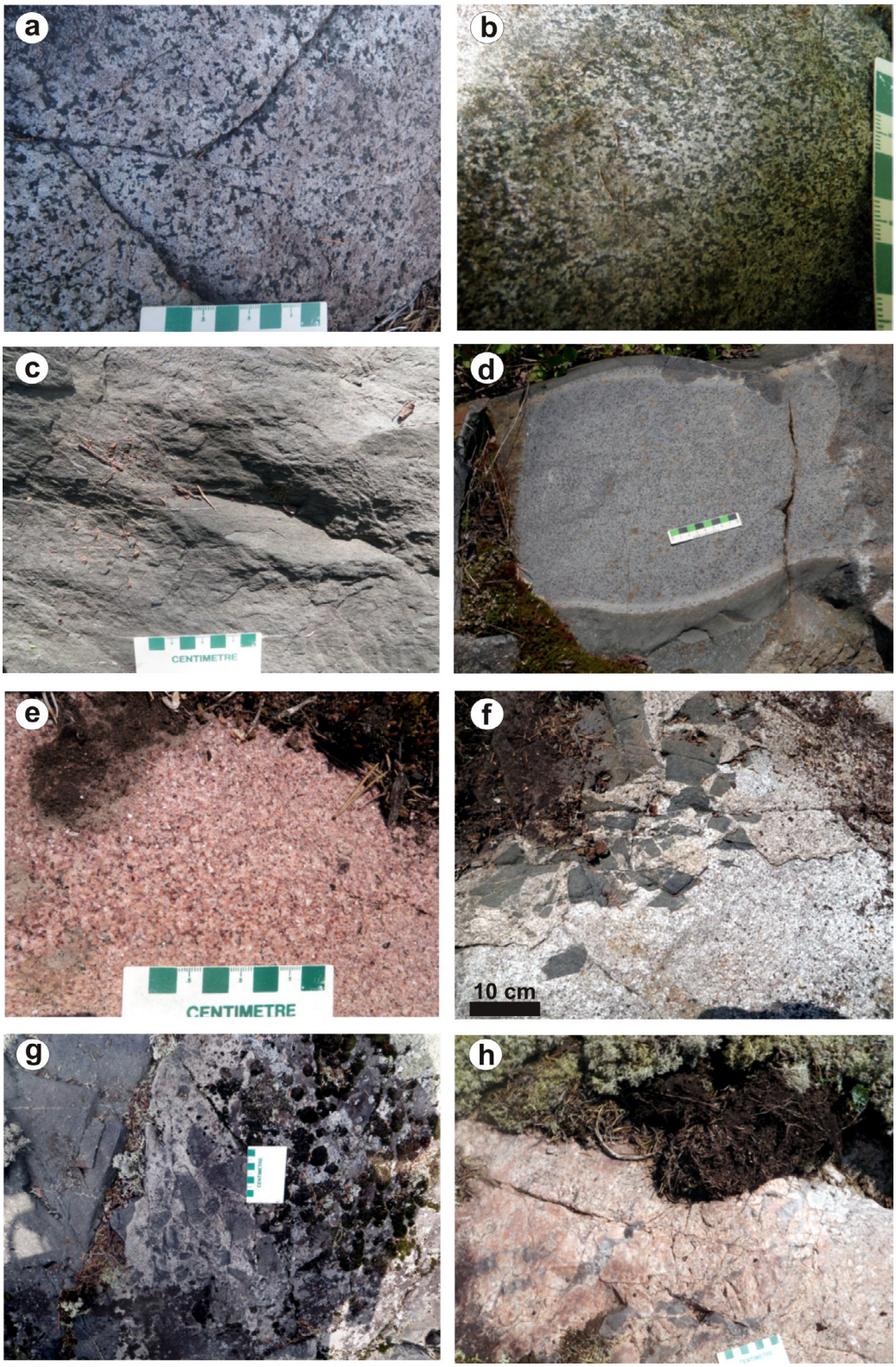

Figure GS-3-6: *Field photographs of map units exhibiting lithological characteristics and/or field relationships (units 7–10 in the Mayville intrusion), Cat Creek area, southeastern Manitoba:* ***a****) coarse-grained leucogabbro (unit 7; UTM Zone 15N, 313722E, 5612269N, NAD83);* ***b****) medium-grained, massive gabbro (unit 8) with notable magnetism (UTM 313138E, 5612992N);* ***c****) fine-grained diabase (unit 9; UTM 315432E, 5612587N);* ***d****) fine-grained quartz diorite dike (unit 10) with chilled margins, cutting pyroxenite and gabbro in the heterolithic breccia zone (UTM 314465E, 5612457N);* ***e****) fine- to medium-grained garnet-muscovite–bearing granite (unit 11b; UTM 310217E, 5613304N);* ***f****) and* ***g****) medium-grained granodiorite (unit 11a) intruding very fine grained basalt (unit 2) and containing basalt fragments (UTM 317746E, 5160077N);* ***h****) pink pegmatite (unit 12; UTM 316185E, 5613722N).*

variations in grain size and/or mineralogical composition. Locally, pegmatitic leucogabbro zones/patches consist of euhedral plagioclase laths and elongate hornblende crystals. The pegmatitic patches are up to 2 m across and have gradational contacts with the surrounding leucogabbro. Near the top of this unit, embayed xenoliths of metasedimentary and fine-grained volcanic rocks occur within the leucogabbro.

Leucogabbro is typically coarse to very coarse grained, locally megacrystic and contains 65–80% calcic plagioclase, 15–25% hornblende (after pyroxene?) and accessory minerals comprising Fe-Ti oxide(s), zircon and apatite. Plagioclase occurs as equant, subhedral to euhedral crystals, without notable optical (or compositional) zoning. At the top of this unit, plagioclase laths display decreasing grain size in a zone that is gradational with the overlying gabbro (see unit 8, below). Hornblende is typically anhedral and interstitial, and locally displays simple twinning. It is unclear whether at least some hornblende is primary or, alternatively, all is of secondary (metamorphic) origin. Sulphide minerals (disseminated pyrite±chalcopyrite) occur locally in sheared zones.

Gabbro (unit 8)

Unit 8 gabbro (Figure GS-3-6b) occurs at the top of the western part of the Mayville intrusion but is apparently absent in the eastern part (east of the Donner Lake Road). The gabbro is massive, equigranular, medium- to coarse-grained and locally strongly magnetic. It consists of 50–60% plagioclase, 30–40% hornblende and accessory magnetite and ilmenite. Plagioclase laths (0.3–0.5 cm long) and subhedral to anhedral hornblende (after pyroxene, 0.2–0.5 cm) locally display ophitic texture. Sericite, chlorite, epidote and biotite alteration are common, especially in fault zones, whereas sulphide minerals are rare.

Diabasic/gabbroic rock (unit 9)

Unit 9 consists of fine- to medium-grained diabasic and gabbroic rocks that occur as dikes and sills in the middle part of the Mayville intrusion. Leucogabbro and anorthosite xenoliths occur locally in diabase intrusions, some of which display chilled margins. These intrusions occur within older leucogabbro (unit 7), as well as metasedimentary rocks (unit 3) north of the Mayville intrusion. The diabase is locally very similar to basalt (unit 2) but is distinguished by its intrusive relationship.

Diabasic and gabbroic rocks are dark green on fresh surface (Figure GS-3-6c) and characterized by plagioclase phenocrysts in a fine-grained matrix of amphibole (after pyroxene) and plagioclase. Chlorite and biotite alteration are common, whereas disseminated pyrrhotite is rare. In most cases, unit 9 rocks are nonmagnetic and appear to be undeformed.

Quartz diorite to tonalite (unit 10)

Quartz diorite to tonalite occurs as undeformed dikes that are characterized by chilled margins (Figure GS-3-6d). At the base of the middle part of the Mayville intrusion (Hititrite occurrence), a southeast-trending, 1.5 m wide quartz diorite dike cuts unit 4 melagabbro. The melagabbro contains up to 7% disseminated pyrrhotite and chalcopyrite, whereas the quartz diorite dike appears to be sulphide free.

Quartz diorite and tonalite are very fine to fine grained and consist mainly of quartz (10–20%) and plagioclase (50–60%), with accessory K-feldspar (<10%), biotite (15%), subhedral hornblende (5%) and minor disseminated magnetite and pyrite. Tiny acicular apatite crystals occur within quartz and plagioclase.

Tonalite, trondhjemite, granodiorite, and late granite (unit 11)

Tonalite, trondhjemite, granodiorite (TTG; unit 11a)

This TTG suite is well exposed south of the eastern part of the Mayville intrusion, where the granitoid rocks intrude unit 2 basalt and related gabbro (Figure GS-3-6f, g). In the central part of the map area, granodiorite (unit 11a) is emplaced in gabbroic rocks of the Mayville intrusion.

The granitoid rocks are medium to coarse grained, massive and locally porphyritic. Feldspar and quartz are the predominant minerals; K-feldspar locally accounts for more than one-third of the total feldspar content and occurs as phenocrysts in porphyritic granodiorite. Biotite±amphibole range from less 10% to 20% in granodiorite, and are typically 10–15%.

Late granodiorite, granite (unit 11b)

Late granodiorite and granite intrusions are closely associated with pink pegmatite bodies that cut all other map units (see below). The late granitoid rocks, which are younger than the Mayville intrusion, occur largely in the area north of the Mayville intrusion; they are rare south of intrusion.

The granitoid rocks (unit 11b) are massive, fine to coarse grained and locally porphyritic; they are only rarely deformed. Quartz, plagioclase and K-feldspar form approximately 90% of the granitoid rocks; muscovite±red garnet±biotite are accessory (Figure GS-3-6e).

Pegmatite (unit 12)

Pegmatite dikes, typically 0.5–15 m thick, are the youngest known intrusive rocks. They occur both to the north and south, and in the central part of the Mayville intrusion. Pegmatite is composed mainly of K-feldspar and quartz (±muscovite±garnet±tourmaline) and displays

graphic textures (Figure GS-3-6h). No deformation or alteration features were observed.

Pegmatites in the BRGB were previously well described by Černý et al. (1981) and were recently revisited by Martins and Kremer (GS-4, this volume).

Lithogeochemical characteristics of the Mayville intrusion and related PGE-Ni-Cu-Cr mineralization

Preliminary geochemical characteristics of the Mayville intrusion were discussed in Yang et al. (2011), based on previously published MGS data in Peck et al. (2000) and Gilbert (2011), as well as some unpublished data from Gilbert. Lacking definitive field relationships, Yang et al. (2011) tentatively concluded, from the available geochemical data, that the Mayville intrusion had been formed from multiple injections of tholeiitic magma(s) derived from partial melting of the upper mantle. These magmas were interpreted to have undergone assimilation and fractional crystallization (AFC) during emplacement in an extensional setting characterized by a thin crust (~21 km). Here we present new analytical data from 17 samples collected mainly from the Mayville intrusion in 2011. Petrographic investigations, chromite chemistry and whole-rock geochemistry and petrogenesis are discussed in terms of their significance for PGE-Ni-Cu-Cr mineralization.

Lithogeochemical features

Table GS-3-1 contains analytical data for 16 rock samples from the Mayville intrusion (units 4–10) and one sample of MORB-type basalt (unit 2); the available geochemical data are consistent with the Mayville intrusion being a composite, relatively evolved mafic–ultramafic intrusion, comparable to Archean megacrystic anorthosite complexes elsewhere (Ashwal, 1993; Peck et al., 2002).

All samples from the Mayville intrusion are tholeiitic (Figure GS-3-7a, b). Two samples that plot in the transitional/calcalkaline fields in Figure GS-3-7b (leucogabbro and pyroxenite, respectively) display higher Th/Yb and Zr/Y ratios, attributed to crustal assimilation. This interpretation is consistent with a positive correlation between these ratios shown in Figure GS-3-7b. Quartz diorite dikes (unit 10) within gabbro of the Mayville intrusion are calcalkaline and appear to be derived from a different source than the mafic–ultramafic rocks.

Chondrite-normalized REE patterns of the major rock types in the Mayville intrusion (Table GS-3-1) are similar to one another. They display flat to slightly positive slopes with moderate to pronounced, positive Eu anomalies, except for a leucogabbro and some melagabbro samples that exhibit negative Eu anomalies attributable to plagioclase fractionation (Figure GS-3-8a). Interestingly, the REE pattern of a basalt sample (unit 2) is coincident with that of mafic–ultramafic rocks in the Mayville intrusion, and also corresponds to that of basalt in the northern MORB-type formation (Gilbert et al., 2008). Individual REE patterns of rocks in the Mayville intrusion are parallel or subparallel, suggesting that the intrusion may have been characterized by multiple batches of magma derived from a common magma chamber where fractional crystallization took place, probably involving all constituent minerals except plagioclase as fractionating phases. One pyroxenite sample displays distinctive light-REE depletion and a slight negative Eu anomaly (Figure GS-3-8a); this rock may either be a cumulate phase or have crystallized from a late phase of ultramafic magma. Field evidence shows that the pyroxenite cuts leucogabbro, thus favouring the latter interpretation.

Two quartz diorite dike samples (Table GS-3-1) exhibit distinctively different REE patterns compared to those of the mafic–ultramafic rocks in the Mayville intrusion (Figure GS-3-8a). They display strong light-REE enrichment and slight Eu anomalies, and have higher La/Yb ratios (≥7) than the mafic–ultramafic rocks (<2.0).

The primitive-mantle–normalized, extended-element diagram (Figure GS-3-8b) also illustrates the distinction between the main phases in the Mayville intrusion and the quartz diorite dikes, which exhibit relatively higher content of high-field-strength elements and pronounced negative Nb anomalies.

A pyroxenite and a leucogabbro sample show pronounced Nb, Ta, Zr and Hf anomalies compared to other samples in the Mayville intrusion (Figure GS-3-8b), which may reflect the presence of accessory phases such as zircon and ilmenite in these samples. Houlé et al. (poster presentation in preparation, 2012) retrieved a significant amount of zircon from one leucogabbro sample that was dated by U-Pb technique.

Yang et al. (2011) used various tectonic discriminant plots, such as Th/Ta versus Yb (Gorton and Schandl, 2000), Zr versus TiO_2 (Syme, 1998) and Th/Nb versus Y (Syme et al., 1999), to investigate the geotectonic setting of the Mayville intrusion. An extensional crustal setting is suggested, likely in an incipient arc-rift environment. The geochemical data (Table GS-3-1) and present mapping support this interpretation; MORB-type basalts and synvolcanic intrusive rocks, as well as the Mayville intrusion, may have been emplaced into an extensional back-arc environment at a continental margin characterized by a relatively thin crust.

Contamination of tholeiitic magma by continental crust would influence the geochemical signature of the magma, because continental rocks have relatively higher $(Th/Yb)_{PM}$[3] (20–100), elevated $(Nb/Yb)_{PM}$ (2–15) and

[3] The subscript 'PM' denotes primitive-mantle-normalized.

Table GS-3-1: Whole-rock geochemistry for the Mayville mafic–ultramafic intrusion, Cat Creek area, southeastern Manitoba.[1]

Sample:	111-11-15	111-11-16	111-11-14	111-11-06	111-11-07	111-11-02	111-11-04	111-11-08	111-11-09
Easting[2]:	314297	314479	314297	315414	315414	316601	316641	315426	315435
Northing[2]:	5612264	5612469	5612264	5612608	5612608	5611951	5611903	5612597	5612598
Rock type:	Anortho-site	Anortho-site	Leuco-gabbro	Leuco-gabbro	Leuco-gabbro	Mela-gabbro	Mela-gabbro	Mela-gabbro	Mela-gabbro
Major elements:[3]									
SiO_2	48.14	46.72	52.70	45.46	48.00	45.51	46.66	40.90	44.23
TiO_2	0.56	0.38	1.34	0.43	0.93	1.01	0.89	0.38	0.54
Al_2O_3	26.02	23.79	13.03	15.03	20.67	13.45	15.69	15.03	14.60
Fe_2O_3(T)	4.79	7.02	13.70	13.97	8.77	17.78	12.28	17.62	15.51
MnO	0.08	0.12	0.16	0.22	0.13	0.20	0.22	0.18	0.19
MgO	3.28	7.01	5.69	10.84	5.93	7.57	9.27	7.55	8.72
CaO	13.00	12.53	10.67	10.55	11.84	9.88	12.42	9.33	10.82
Na_2O	2.50	1.52	1.21	1.21	2.25	1.89	0.90	1.14	1.40
K_2O	0.32	0.23	0.19	0.16	0.18	0.18	0.76	0.10	0.10
P_2O_5	0.05	0.03	0.40	0.04	0.07	0.07	0.08	0.03	0.02
LOI	1.13	0.88	0.74	1.14	0.78	2.15	0.87	4.01	1.52
Total	99.87	100.20	99.81	99.05	99.55	99.70	100.00	96.27	97.64
S	0.06	0.03	< 0.01	0.77	0.08	3.05	0.03	5.42	2.14
Trace elements:[4]									
V	146	93	168	150	233	347	287	127	235
Cr	200	90	< 20	150	140	230	280	120	240
Co	15	31	64	87	28	134	38	113	88
Ni	120	220	120	900	170	1660	230	1580	1060
Cu	340	150	20	980	550	4260	110	> 10000	2510
Zn	40	50	< 30	120	70	110	90	110	80
Ga	19	16	14	14	18	15	17	13	14
Rb	2	4	< 1	< 1	2	< 1	29	2	1
Sr	284	138	230	62	168	76	76	107	70
Y	10.2	6.4	17.8	9.5	17.3	21.3	18.6	8.9	10.2
Zr	38	12	204	23	38	33	37	27	21
Nb	1.1	0.5	5.4	0.9	2.1	1.8	1.9	0.8	0.8
Mo	< 2	< 2	< 2	< 2	< 2	< 2	< 2	< 2	< 2
Ag	< 0.5	< 0.5	< 0.5	< 0.5	< 0.5	0.9	< 0.5	0.8	< 0.5
Cs	1.7	2.2	0.9	0.4	0.8	0.2	2.6	0.4	0.3
Ba	27	50	39	20	48	25	97	14	21
La	2.05	1.23	2.21	1.68	2.61	2.82	2.30	1.77	1.40
Ce	4.54	2.97	3.99	4.77	7.09	7.56	6.82	4.28	3.81
Pr	0.65	0.43	0.58	0.70	1.11	1.20	1.09	0.64	0.58
Nd	3.48	2.50	3.63	3.78	6.25	6.82	6.25	3.20	3.23
Sm	1.16	0.80	1.51	1.16	2.23	2.47	2.20	1.03	1.18
Eu	0.49	0.42	0.28	0.59	0.68	0.75	0.68	0.46	0.49
Gd	1.46	0.96	2.31	1.42	2.65	3.23	2.91	1.29	1.49
Tb	0.28	0.17	0.43	0.26	0.50	0.62	0.53	0.25	0.28
Dy	1.82	1.15	2.86	1.71	3.27	3.93	3.43	1.63	1.86
Ho	0.40	0.25	0.64	0.37	0.67	0.82	0.72	0.36	0.40
Er	1.23	0.76	1.98	1.11	2.03	2.47	2.22	1.05	1.24
Tm	0.18	0.11	0.31	0.17	0.30	0.36	0.33	0.16	0.18
Yb	1.18	0.74	2.15	1.14	2.01	2.39	2.15	1.06	1.20
Lu	0.19	0.11	0.36	0.19	0.31	0.37	0.33	0.17	0.19
Hf	1.1	0.3	5.8	0.7	1.1	0.9	1.1	0.7	0.6
Ta	0.08	0.03	0.62	0.03	0.15	0.12	0.13	0.05	0.03
Pb	6	6	5	5	6	6	5	6	6
Bi	< 0.1	< 0.1	< 0.1	0.2	< 0.1	0.2	0.1	0.2	0.2
Th	0.16	0.06	0.61	0.15	0.26	0.17	0.24	0.15	0.13
U	0.05	0.02	0.14	0.05	0.07	0.05	0.06	0.04	0.03
Pd	< 1	33	< 1	103	6	192	4	192	206
Pt	< 1	20	< 1	33	5	47	6	32	76
Au	4	3	< 2	13	13	51	< 2	46	39

[1] Analyses carried out by Actlabs, Ancaster, Ontario, using the 4E Research package to analyze bulk-rock compositions, and fire assay-ICP/MS to analyze precious metals (Pd, Pt, Au), and infrared spectrometry for S.
[2] UTM Zone 15N, NAD 83
[3] Major-element concentrations are in weight percent.
[4] Trace-element concentrations are in ppm, except for Pd, Pt and Au, which are in ppb.

Table GS-3-1: Whole-rock geochemistry for the Mayville mafic–ultramafic intrusion, Cat Creek area, southeastern Manitoba.[1] *(continued)*

Sample:	111-11-10	111-11-11	111-11-12	111-11-17	111-11-01	111-11-03	111-11-05	111-11-13
Easting[2]:	315438	314320	314287	314200	314202	314091	316626	314309
Northing[2]:	5612598	5612292	5612272	5612542	5612535	5612056	5611931	5612274
Rock type:	Mela-gabbro	Pyroxenite	Pyroxenite	Pyroxenite	Pyroxenite	Basalt	Quartz diorite	quartz diorite
Major elements:[3]								
SiO_2	50.44	42.38	40.98	46.43	42.41	50.14	65.69	58.09
TiO_2	0.77	0.54	0.48	1.32	0.18	0.78	0.52	0.87
Al_2O_3	15.18	15.78	15.72	15.11	12.33	14.11	15.31	15.47
Fe_2O_3(T)	11.78	12.00	12.45	12.34	12.70	12.55	5.94	10.16
MnO	0.19	0.16	0.17	0.22	0.17	0.24	0.07	0.17
MgO	8.19	13.70	14.84	10.25	19.82	7.86	2.67	4.95
CaO	11.96	11.00	9.78	11.61	7.01	11.38	4.48	7.26
Na_2O	1.53	1.91	1.40	1.15	0.53	2.07	3.28	3.41
K_2O	0.09	0.23	0.16	0.16	0.05	0.31	1.47	0.11
P_2O_5	0.03	0.05	0.06	0.02	0.01	0.06	0.12	0.16
LOI	0.69	1.64	3.06	1.19	5.15	0.58	0.69	0.24
Total	100.80	99.39	99.10	99.79	100.40	100.10	100.20	100.90
S	0.03	0.07	0.02	0.02	0.03	< 0.01	0.02	0.04
Trace elements:[4]								
V	300	117	104	157	118	293	94	213
Cr	270	490	480	190	390	230	50	30
Co	39	54	56	41	75	43	14	27
Ni	140	440	390	340	780	130	50	60
Cu	150	240	240	30	100	20	100	80
Zn	60	70	50	50	40	70	70	80
Ga	15	12	12	13	10	15	18	17
Rb	1	< 1	< 1	1	< 1	2	50	< 1
Sr	79	41	49	114	41	96	194	214
Y	12.7	12.8	11.8	14.3	4.2	16.5	12.7	16
Zr	23	39	32	136	7	41	139	97
Nb	0.7	1.6	1.4	4.7	< 0.2	1.5	5.3	4.5
Mo	< 2	< 2	< 2	< 2	< 2	< 2	< 2	< 2
Ag	< 0.5	< 0.5	< 0.5	< 0.5	< 0.5	< 0.5	< 0.5	< 0.5
Cs	0.2	0.2	0.2	0.6	0.2	0.2	1.8	< 0.1
Ba	20	31	32	28	15	78	353	97
La	1.32	2.15	2.26	1.38	0.65	2.35	16.60	12.60
Ce	3.84	5.95	5.50	5.71	1.46	6.86	33.10	26.70
Pr	0.60	0.92	0.81	1.15	0.22	1.08	3.69	3.19
Nd	3.67	4.97	4.28	7.17	1.21	6.11	14.30	13.60
Sm	1.31	1.63	1.47	2.13	0.44	1.94	2.87	2.98
Eu	0.57	0.61	0.59	0.75	0.20	0.78	0.75	1.07
Gd	1.70	1.98	1.87	2.18	0.48	2.48	2.33	2.91
Tb	0.35	0.38	0.35	0.40	0.10	0.46	0.38	0.48
Dy	2.38	2.32	2.16	2.60	0.71	2.97	2.37	2.91
Ho	0.52	0.51	0.47	0.56	0.16	0.64	0.48	0.60
Er	1.56	1.50	1.38	1.73	0.53	1.96	1.42	1.84
Tm	0.24	0.23	0.21	0.27	0.08	0.29	0.21	0.27
Yb	1.54	1.45	1.35	1.84	0.58	1.90	1.45	1.79
Lu	0.24	0.22	0.21	0.31	0.10	0.30	0.24	0.28
Hf	0.7	1.1	0.9	3.5	0.2	1.1	3.3	2.3
Ta	0.03	0.1	0.11	0.37	< 0.01	0.09	0.54	0.37
Pb	6	5	5	5	5	5	8	6
Bi	0.1	< 0.1	< 0.1	< 0.1	< 0.1	< 0.1	< 0.1	< 0.1
Th	0.12	0.19	0.15	0.16	< 0.05	0.24	4.5	2
U	0.03	0.06	0.07	0.04	< 0.01	0.06	1.15	0.47
Pd	6	< 1	3	14	86	4	< 1	< 1
Pt	10	2	6	3	20	8	< 1	< 1
Au	< 2	5	4	< 2	4	< 2	< 2	< 2

[1] Analyses carried out by Actlabs, Ancaster, Ontario, using the 4E Research package to analyze bulk-rock compositions, and fire assay-ICP/MS to analyze precious metals (Pd, Pt, Au), and infrared spectrometry for S.
[2] UTM Zone 15N, NAD 83
[3] Major-element concentrations are in weight percent.
[4] Trace-element concentrations are in ppm, except for Pd, Pt and Au, which are in ppb.

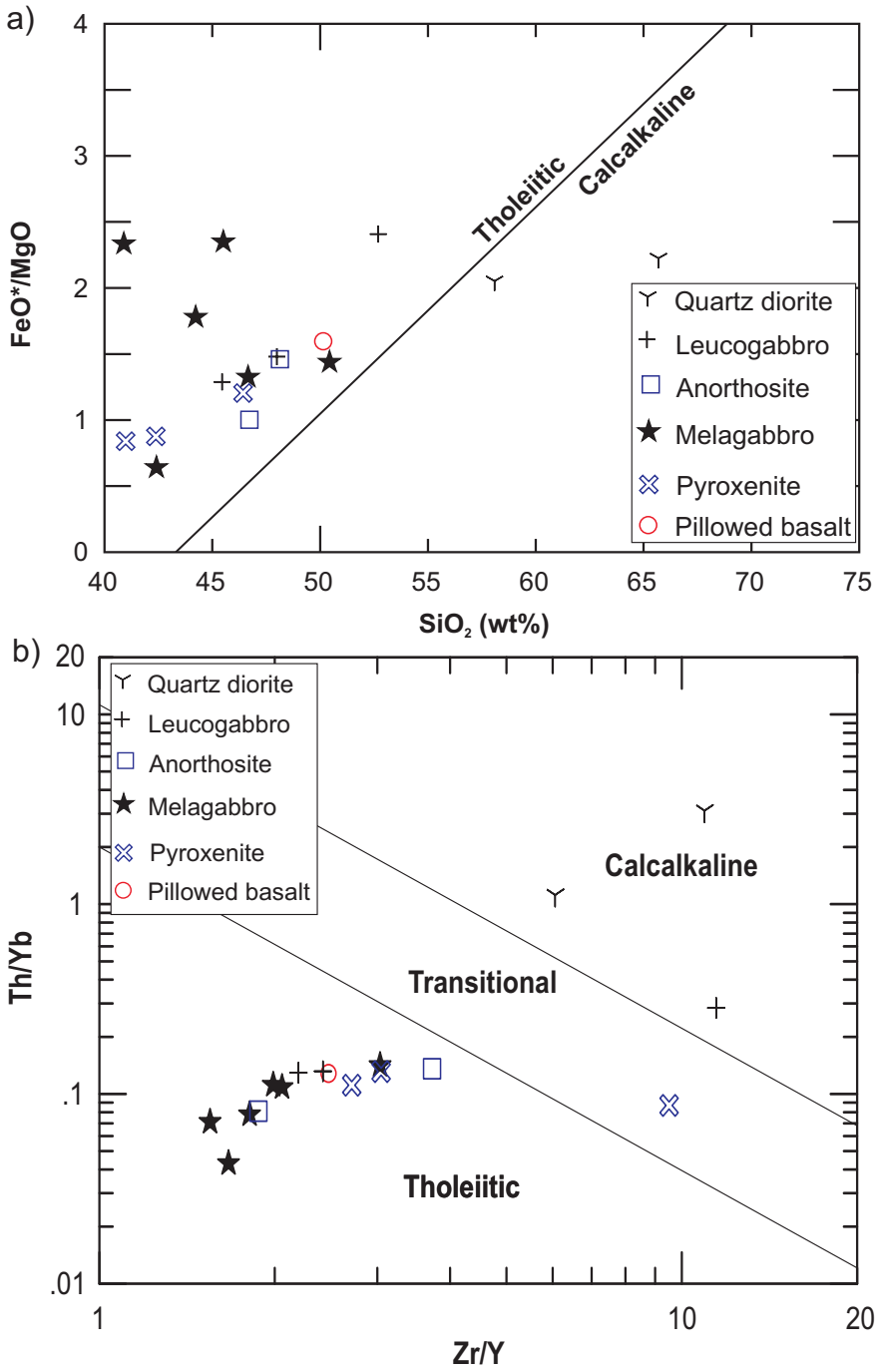

Figure GS-3-7: *Discrimination diagrams for rocks of the Mayville mafic–ultramafic intrusion, Cat Creek area, southeastern Manitoba:* ***a)*** *FeO^T/MgO versus SiO_2 (wt. %; boundary between tholeiitic and calcalkaline rock series from Miyashiro, 1974);* ***b)*** *Th/Yb versus Zr/Y (boundaries between tholeiitic, transitional and calcalkaline from Ross and Bédard, 2009).*

greater Th enrichment relative to Nb compared to juvenile magma (Lightfoot et al., 1990; Keays and Lightfoot, 2010; Yuan et al., 2012). A geochemical model of simple mixing between N-MORB magma and upper continental crust was carried out to test the hypothesis that the Mayville intrusion was emplaced in an extensional environment at a continental margin (Figure GS-3-9a, b). The model suggests that about 5–10% contamination by continental crust is required to elevate the $(Th/Yb)_{PM}$, $(Nb/Yb)_{PM}$ and $(Th/Nb)_{PM}$ ratios in N-MORB magmas to the values observed in the Mayville intrusion. This contamination is thought to be important for triggering sulphide saturation in tholeiitic magmas (Naldrett, 2004). In the case of the Mayville intrusion, a source for contamination (and addition of external sulphur) that could have resulted in sulphide saturation has not yet been identified. One possible candidate—unit 3 metasedimentary rocks north and west of the Mayville intrusion—does not

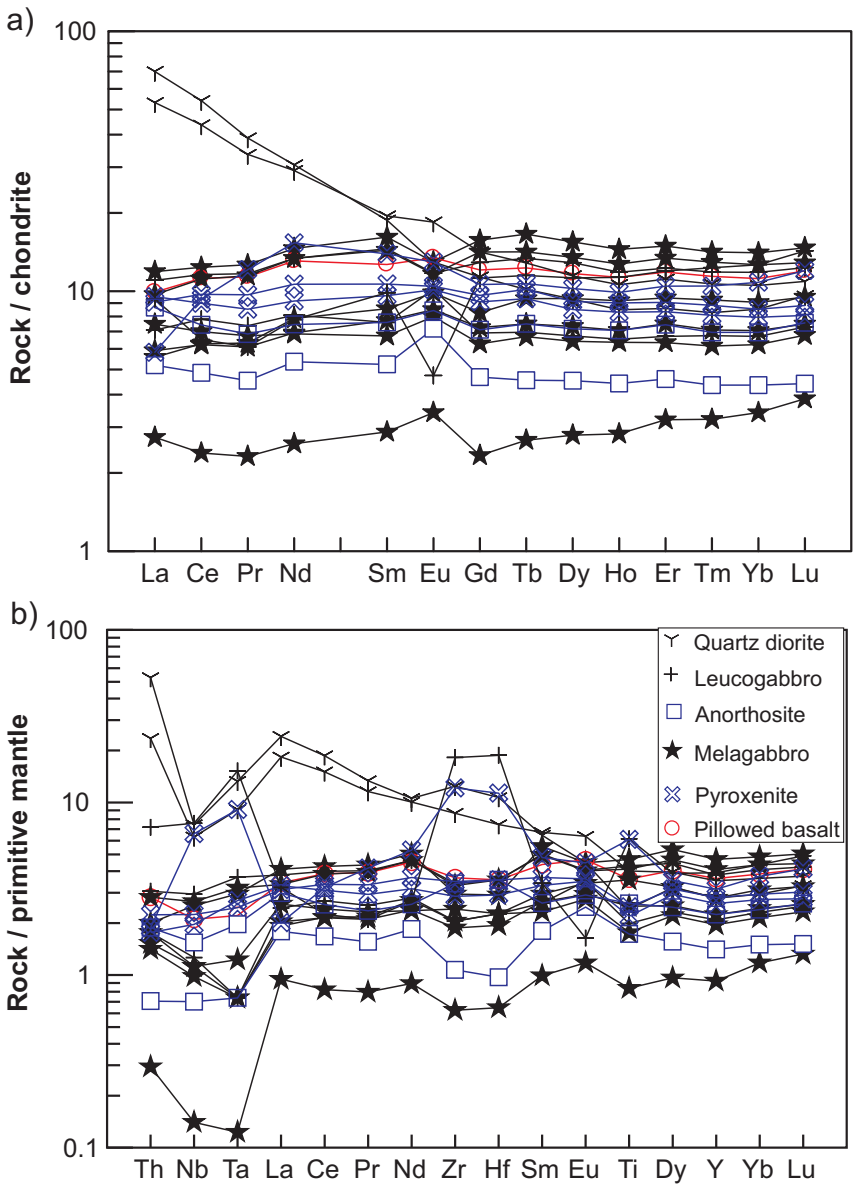

Figure GS-3-8: *Chondrite-normalized REE diagram* ***(a)****, and primitive-mantle–normalized extended element diagram* ***(b)*** *for the various rock types (Table GS-3-1) of the Mayville intrusion, Cat Creek area, southeastern Manitoba. Normalizing values from Sun and McDonough (1989).*

appear to contain appreciable amounts of sulphide/sulphate minerals, which are key to initiating sulphur saturation in mineralized mafic–ultramafic systems (e.g., Keays and Lightfoot, 2010).

Quartz diorite samples (unit 10) display high $(Th/Nb)_{PM}$ ratios (3.68–7.03) and $(Nb/Yb)_{PM}$ ratios (2.45–3.68; Figure GS-3-9b, Table GS-3-1), suggesting that they may have been derived dominantly from partial melting of a continental-crust source and are thus unlikely comagmatic with the Mayville intrusion.

Chemical composition of chromite

Massive, fine-grained chromitite consists of euhedral and subhedral to anhedral chromite, (0.02–0.3 mm in diameter, 35–50 modal %) in a groundmass of serpentine and chlorite material (Figure GS-3-10a). Most chromite grains are unaltered, but some display minor chloritic alteration. Compositional zoning is common, mostly with an FeO^T-enriched rim and Cr_2O_3-rich core; however, reverse zoning is also present. Opaque minerals are dominantly chromite (Figure GS-3-10b) and lesser ilmenite.

Disseminated chromite occurs in pyroxenite and gabbroic rocks of the Mayville intrusion. Pyroxenite is commonly coarse grained, showing adcumulus texture, and consists dominantly of hornblende (as a result of alteration of pyroxene, mostly clinopyroxene). Hornblende crystals are euhedral to subhedral and >90% in mode. Some hornblende grains are strongly altered to chlorite,

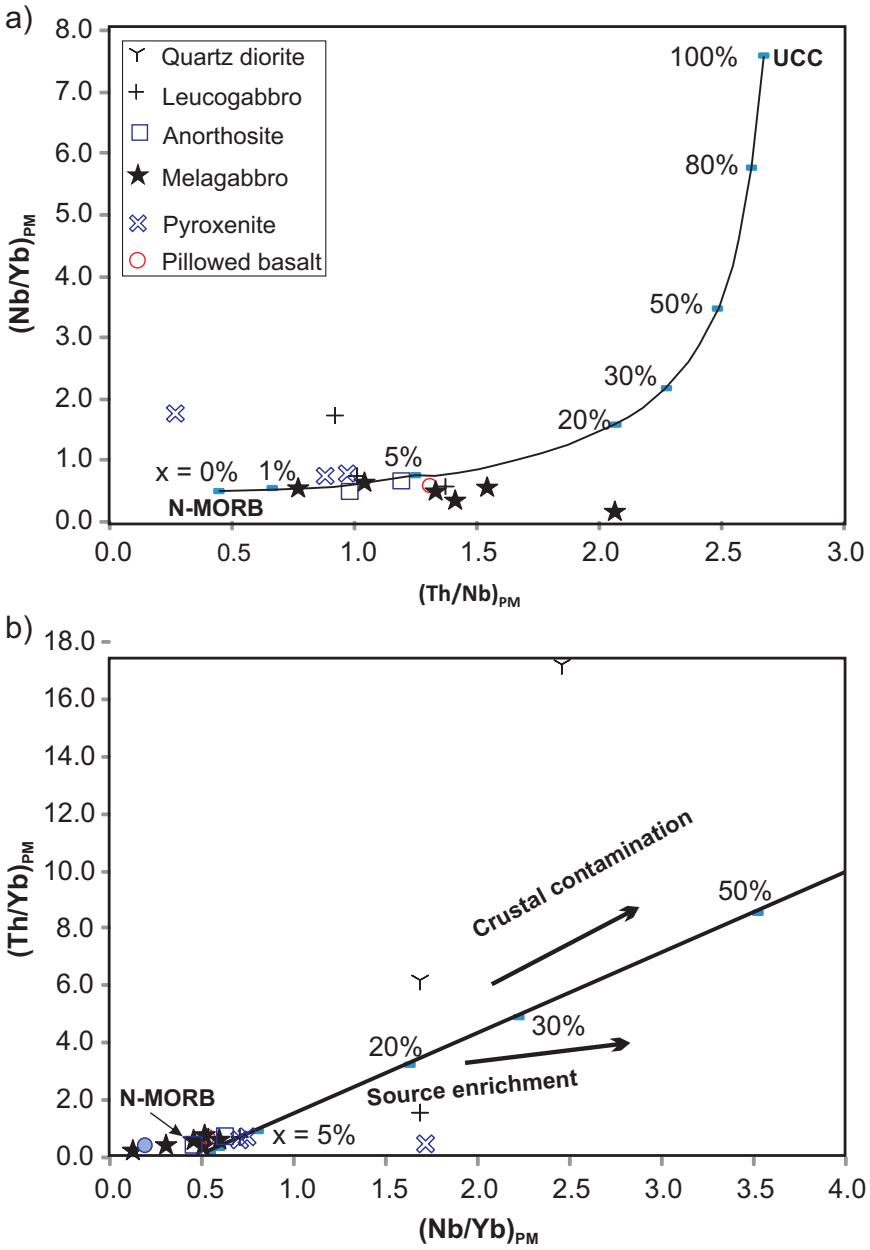

Figure GS-3-9: *Plot of primitive-mantle–normalized $(Th/Nb)_{PM}$ versus $(Nb/Yb)_{PM}$* ***(a)*** *and $(Nb/Yb)_{PM}$ versus $(Th/Yb)_{PM}$* ***(b)*** *for mafic rocks of the Mayville intrusion, Cat Creek area, southeastern Manitoba. The mixing curve is between normal mid-ocean-ridge basalt (N-MORB) and the upper continental crust (UCC). The variable 'x' is the percentage of UCC assimilated by mafic magma with an N-MORB composition. Data for N-MORB and UCC composition are from Taylor and McLennan (1985). Primitive-mantle values are from McDonough and Sun (1995). Trends of source enrichment and crustal contamination are from Yuan et al. (2012).*

carbonate and magnetite. Recrystallization along some grains is manifested by smaller amphibole aggregates. Disseminated chromite occurs as inclusions in hornblende grains, and sulphide minerals (e.g., pyrite and pyrrhotite) are interstitial (Figure GS-3-10c, d).

On the Cr-Al-Fe ternary diagram, two populations of chromite in the Mayville intrusion are present. One group of data displays an Fe-Ti trend and exhibits characteristics of enriched Fe^{3+}; the other group, together with the data from the BRS, displays a Rum trend (i.e., an increase in Al^{3+} mainly at the expense of Cr^{3+} with some decrease in Fe^{3+}, accompanied by decreasing $Fe^{2+}/(Mg + Fe^{2+})$, as shown in Figure GS-3-11a, indicating their similarities in terms of chromite chemistry. This suggests that the chemistry of chromite reflects the parental magmas from which it may have differentiated through fractionation in a continental-crust setting. It is interpreted that this combined trend is a result of reaction between cumulus chromite

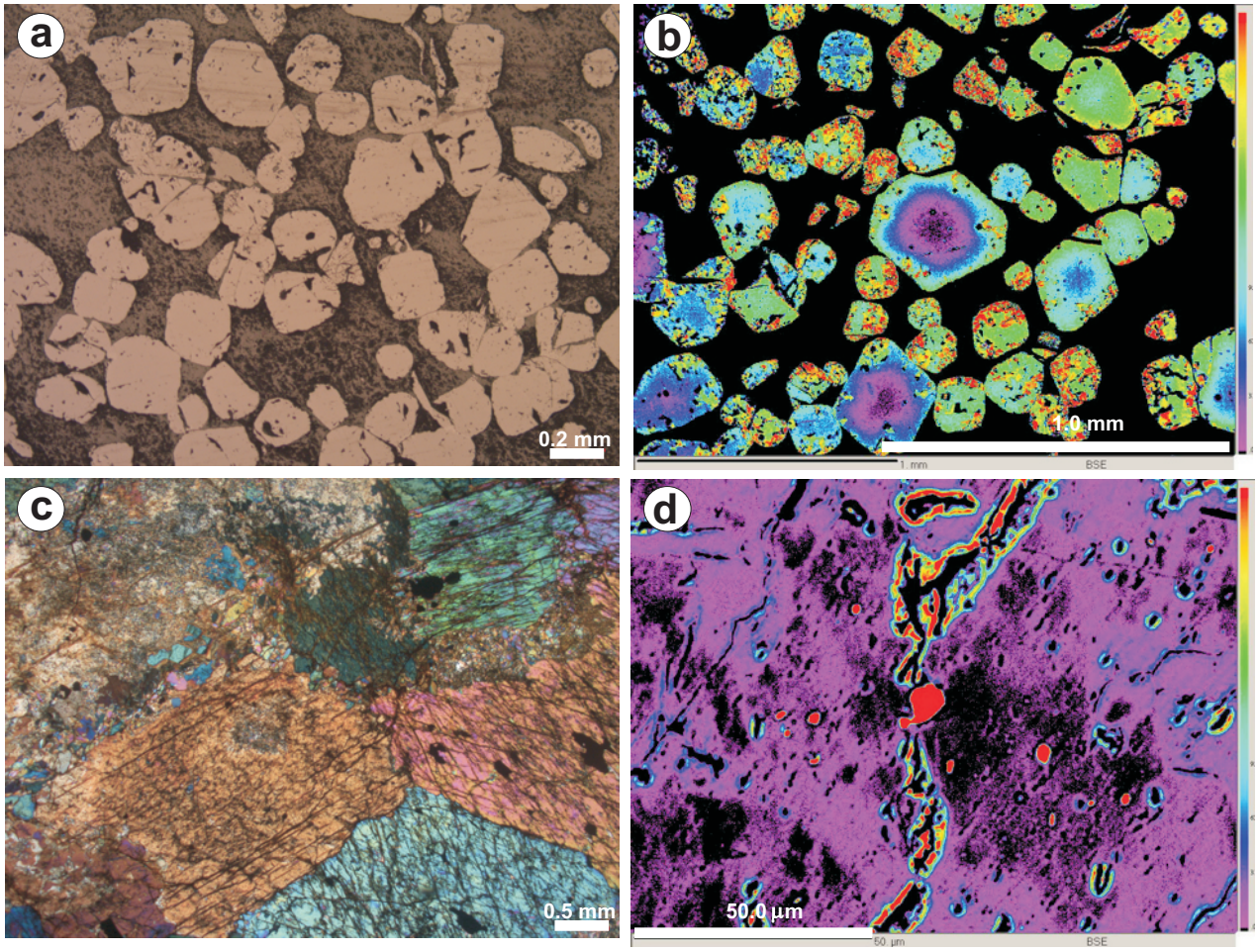

Figure GS-3-10: *Chromite textures in chromitite of the Bird River Sill (a, b) and in pyroxenite of the Mayville intrusion (c, d), Cat Creek area, southeastern Manitoba:* ***a****) euhedral to subhedral chromite grains in groundmass of serpentine and chlorite (sample 111-11-20), reflected-polarized light (RPL);* ***b****) compositional zoning of chromite (sample 111-11-20), shown in back-scattered electron (BSE) image with pseudo-colours, disrupted chromitite bands;* ***c****) coarse-grained pyroxenite in the Mayville intrusion (sample 111-11-12) containing hornblende, with chlorite and carbonate alteration and chromite inclusion, cross-polarized light; and* ***d****) chromite inclusions (red) in hornblende (formerly clinopyroxene; sample 111-11-12), BSE image.*

crystals and evolving interstitial silicate melt, consistent with the observations of Barnes and Roeder (2001). They pointed out that a Rum trend is commonly restricted to mafic layered intrusions, attributed to reaction between cumulus chromite, trapped intercumulus liquid, plagioclase and olivine.

Some of the chromite in chromitites from the BRS has a relatively low Fe^{3+} content (Figure GS-3-11a). Because the ratio of chromite to trapped liquid is so high in chromitite, the effect of reaction between chromite and interstitial liquid on the composition of chromite may be less pronounced. Thus, chromitite likely reflects the primary composition of liquidus chromite.

On a plot of Cr-number (Cr/Cr + Al) versus Fe-number (Figure GS-3-11b), chromite from the Mayville intrusion forms a continuous trend with chromite in Archean anorthosite complexes of Rollinson et al. (2010), but is distinct from that in chromitites from the BRS. The Mayville chromite displays variable Cr-numbers, but relatively narrow and higher Fe-numbers. The BRS chromite has relatively constant Cr-numbers, but variable and lower Fe-numbers. At a fixed Cr-number, the Mayville chromite has a higher Fe-number than the BRS chromite, which formed from relatively primitive (i.e., higher Mg-number) magma(s), consistent with their geochemical signatures.

The Mayville intrusion is more evolved, as evidenced by chromite with higher Al/Cr ratios and lower Mg-numbers (Mg/Mg + Fe^{2+}) than those of chromite from the BRS. A preliminary U-Pb zircon age (2743 Ma) for the Mayville intrusion (V. McNicoll, pers. comm., 2012) indicates that it is contemporaneous with the 2744.7 ±5.2 Ma BRS (Wang, 1993), suggesting that the two intrusions were products of the same mafic-ultramafic magmatism during Neoarchean time.

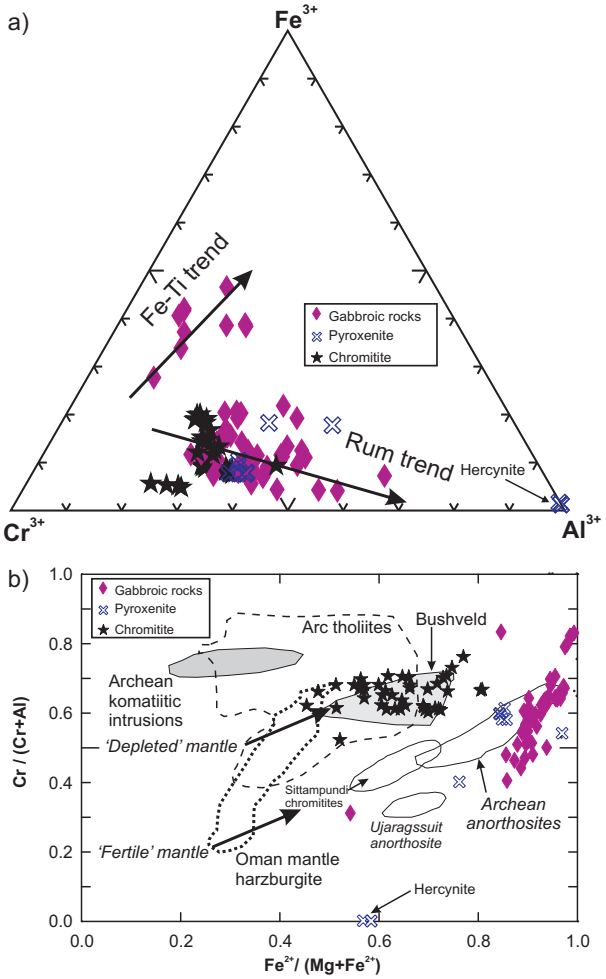

Figure GS-3-11: a) *Ternary diagram of trivalent cation Cr-Al-Fe in chromite from the Mayville intrusion and the Bird River Sill (BRS; indicated by black stars), Cat Creek area, southeastern Manitoba. Data sources are this study, Gait (1964) and Hiebert (2003). Arrows show the Fe-Ti trend and Rum trend (Barnes and Roeder, 2001);* ***b****) Plot of Fe-number versus Cr-number of chromite from the Mayville intrusion and BRS. Data sources are this study, Gait (1964) and Hiebert (2003). Hercynite has the lowest Cr-number (= 0). Fields of chromite in arc tholeiite are from Barnes and Roeder (2001); in the Oman ophiolite (from the 'fertile' mantle harzburgite; dotted outline) is from Le Mée et al. (2004); and in Archean komatiitic intrusions, Bushveld, Archean anorthosites, Ujaragssuit anorthosite and Sittampundi chromitite are from Rollinson et al. (2010). The coarse arrows show the evolution of melts from aluminous (fertile) mantle in the Archean and from less aluminous (depleted) mantle in modern arcs (after Rollinson et al., 2010).*

Features of PGE-Ni-Cu-Cr mineralization associated with the Mayville intrusion

Field mapping, diamond-drilling and lithogeochemical data (Table GS-3-1) indicate that three styles of magmatic sulphide mineralization occur within the Mayville intrusion (Peck et al., 2002; Yang et al., 2011):

- Contact-style, magmatic Ni-Cu-PGE mineralization at the base of the intrusion (e.g., M2 deposit, Hititrite occurrence)
- Reef-style, stratiform, magmatic PGE-Ni-Cu-Cr mineralization (e.g., PGE zone)
- PGE mineralization in a transitional zone and/or contact zones of different phases (e.g., melagabbro-pyroxenite contact in the HBX)

These observations are consistent with primary sulphide minerals in the Mayville mafic–ultramafic rocks. Contents of Ni, Cu and PGEs correlate positively with S and/or sulphide content in the mafic–ultramafic rock samples from the Mayville intrusion (Table GS-3-1; Peck et al., 1999; Mustang Minerals Corp., 2011; Yang et al., 2011). Reef-style, stratiform, magmatic PGE-Ni-Cu-Cr mineralization within the Mayville intrusion is consistent with a mineralization style analogous to the stratabound PGE-enriched sulphide- and chromite-bearing layers described by Hoatson (1998). However, the enrichment mechanism of PGEs in a transitional zone and/or contact zone of different phases related to the injection of new batches of mafic–ultramafic melt(s), especially replenishment of ultramafic magmas, requires further investigation.

The rock compositions may have been influenced by postmineralization structures (e.g., north-northeast- and north-northwest-trending shear zones) that could have remobilized the primary sulphide ores. Such cases are not uncommon in the BRS magmatic sulphide mineralization systems (e.g., Murphy and Theyer, 2005; Mealin, 2008; Good et al., 2009) and in the Thompson Belt Ni deposits (Bleeker and Macek, 1996). Therefore, structural analysis is important to localize sulphide Ni-Cu-PGE ores in the mafic–ultramafic system that was influenced by tectonism.

Economic considerations

The Cat Creek area contains several Archean layered mafic–ultramafic intrusions similar to those that host significant Ni-Cu-PGE-Cr mineralization worldwide. Current mapping and lithogeochemical studies suggest that the Mayville intrusion formed from multiple injections of alumina-rich tholeiitic magma derived from high-degree partial melting of a subcontinental lithospheric mantle source; during the emplacement process of each batch magma, assimilation and fractional crystallization may have played an important role in petrogenesis, which may have triggered sulphide saturation, subsequent liquidation and mineralization. Cooling of the intrusion appears to have occurred from north to south, regardless of replenishment by new batches mafic–ultramafic magma(s) into the chamber. The continuity of the heterolithic breccia zone (HBX) in the Mayville intrusion suggests a dynamic system favourable for formation of magmatic sulphide Ni-Cu-PGE-Cr mineralization.

The Mayville intrusion, the largest in the area, hosts a significant amount of Ni-Cu-PGE mineralization in the M2 deposit, recognized as contact-style magmatic sulphide mineralization. At M2, the sulphide-rich mineralization is typically located near the base of the HBX and basal contact of the intrusion, whereas disseminated sulphide minerals are widespread throughout the HBX and basal mafic–ultramafic rocks. Furthermore, other styles of mineralization, such as reef-style, stratiform PGE mineralization and stratiform chromitite mineralization, also occur in the Mayville intrusion. The transitional and/or contact zones between major rock units may be particularly enriched in PGEs. In addition to Ni-Cu-PGE sulphide mineralization, the Mayville intrusion may host significant chromite mineralization, as suggested by the presence of massive chromitite bands and disrupted chromitite-pyroxenite layers within the HBX.

Investigation of the magmatic architecture of the Mayville intrusion via the physical properties of the intrusive magma and the surrounding rocks, together with structural and geophysical analysis, may assist in interpreting the mechanism(s) of emplacement (e.g., Houlé et al., 2008), as well as identifying potential locations of feeder and/or magma conduit(s).

It is noteworthy that Archean anorthosite complexes, including the Mayville intrusion, host potential industrial-mineral resources for producing aluminum chemicals via acid processes. Aluminum chemicals are utilized variously as industrial coatings, fillers, absorbent materials and cement additives (Veldhuyzen, 1995).

Acknowledgments

We thank L. Lafreniere (University of Manitoba), M. Hamilton (Brandon University), C. Boudreau (Université Laval) and C. Böhm for assistance in the field. We are grateful to Mustang Minerals Corp. for providing access to their property, drillcore and geological database, particularly C. Galeschuk, J. Fulton-Regula and A. Dietz for their generous assistance and constructive discussion. P.D. Kremer and M.T. Corkery are thanked for discussion of regional geology of the Bird River greenstone belt. R. Sidhu and A. Camacho at the University of Manitoba are gratefully thanked for assistance with electron microprobe analysis. We thank G. Keller and P. Lenton for technical support; L. Chackowsky, B. Lenton and M. McFarlane for providing GIS data, digitizing the map data and drafting figures; M. Pacey for assembling the digital database for a hand-held data acquisition system; L. Janower and E. Hunter for locating some key references; and G. Benger, R. Unruh and V. Varga for handling the samples and preparing polished thin sections. N. Brandson and E. Anderson are thanked for assembling field equipment and providing expediting services. Constructive reviews of the manuscript by P. Kremer and C. Böhm are gratefully acknowledged.

References

Anderson, S.D. 2007: Stratigraphic and structural setting of gold mineralization in the Lily Lake area, Rice Lake greenstone belt, Manitoba (NTS 52L11, 14); *in* Report of Activities 2007, Manitoba Science, Technology, Energy and Mines, Manitoba Geological Survey, p. 114–128.

Anderson, S. D. 2008: Geology of the Rice Lake area, Rice Lake greenstone belt, southeastern Manitoba (parts of NTS 52L13, 52M4); Manitoba Science, Technology, Energy and Mines, Manitoba Geological Survey, Geoscientific Report GR2008-1, 96 p.

Ashwal, L.D. 1993: Anorthosites; Springer-Verlag, Berlin, Germany, 422 p.

Bailes, A.H., Percival, J.A., Corkery, M.T., McNicoll, V.J., Tomlinson, K.Y., Sasseville, C., Rogers, N., Whalen, J.B. and Stone, D. 2003: Geology and tectonostratigraphic assemblages, West Uchi map area, Manitoba and Ontario; Manitoba Geological Survey, Open File OF2003-1, Geological Survey of Canada, Open File 1522, Ontario Geological Survey, Preliminary Map P.3461, 1:250 000 scale.

Barnes, S.J. and Roeder, P.L. 2001: The range of spinel compositions in terrestrial mafic and ultramafic rocks; Journal of Petrology, v. 42, p. 2279–2302.

Beaumont-Smith, C.J., Anderson, S.D., Bailes, A.H. and Corkery, M.T. 2003: Preliminary results and economic significance of geological mapping and structural analysis at Sharpe Lake, northern Superior Province, Manitoba (parts of NTS 53K5 and 6); *in* Report of Activities 2003, Manitoba Industry, Economic Development and Mines, Manitoba Geological Survey, p. 140–158.

Bleeker, W. and Macek, J.J. 1996: Evolution of the Thompson Nickel Belt, Manitoba: setting of Ni-Cu deposits in the western part of the circum Superior boundary zone; Geological Association of Canada–Mineralogical Association of Canada, Joint Annual Meeting, Winnipeg, Manitoba, Field Trip Guidebook A1, 45 p.

Böhm, C.O., Heaman, L.M., Creaser, R.A. and Corkery, M.T. 2000: Discovery of pre–3.5 Ga exotic crust at the northwestern Superior Province margin, Manitoba; Geology, v. 28, p. 75–78.

Burke, K. 2011: Plate tectonics, the Wilson cycle, and mantle plumes: geodynamics from the top; Annual Review of Earth and Planetary Sciences, v. 39, p. 1–29.

Černý, P., Trueman, D.L., Ziehlke, D.V., Goad, B.E. and Paul, B.J. 1981: The Cat Lake–Winnipeg River and the Wekusko Lake pegmatite fields, Manitoba; Manitoba Energy and Mines, Mineral Resources Division, Economic Geology Report ER80-1, 216 p.

Corkery, M.T., Murphy, L.A. and Zwanzig, H.V. 2010: Re-evaluation of the geology of the Berens River Domain, east-central Manitoba (parts of NTS 52L, M, 53D, E, 62P, 63A, H); *in* Report of Activities 2010, Manitoba Innovation, Energy and Mines, Manitoba Geological Survey, p. 135–145.

Duguet, M., Lin, S., Davis, D.W., Corkery, M.T. and McDonald, J. 2009: Long-lived transpression in the Archean Bird River greenstone belt, western Superior Province, southeastern Manitoba; Precambrian Research, v. 174, no. 3–4, p. 381–407.

Gait, R.I. 1964: The mineralogy of the chrome spinels of the Bird River Sill, Manitoba; M.Sc. thesis, University of Manitoba, Winnipeg, Manitoba, 64 p.

Gilbert, H.P. 2006: Geological investigations in the Bird River area, southeastern Manitoba (parts of NTS 52L5N and 6); *in* Report of Activities 2006, Manitoba Science, Technology, Energy and Mines, Manitoba Geological Survey, p. 184–205.

Gilbert, H.P. 2007: Stratigraphic investigations in the Bird River greenstone belt, Manitoba (part of NTS 52L5, 6); *in* Report of Activities 2007, Manitoba Science, Technology, Energy and Mines, Manitoba Geological Survey, p. 129–143.

Gilbert, H.P. 2008: Geology of the west part of the Bird River area, southeastern Manitoba (NTS 52L5); Manitoba Science, Technology, Energy and Mines, Manitoba Geological Survey, Preliminary Map PMAP2008-6, scale 1:20 000.

Gilbert, H.P. and Kremer, P.D. 2008: Geology of the east part of the Bird River area, southeastern Manitoba (NTS 52L6); Manitoba Science, Technology, Energy and Mines, Manitoba Geological Survey, Preliminary Map PMAP2008-5, scale 1:20 000.

Gilbert, H.P., Davis, D.W., Duguet, M., Kremer, P.D., Mealin, C.A. and MacDonald, J. 2008: Geology of the Bird River Belt, southeastern Manitoba (parts of NTS 52L5, 6); Manitoba Science, Technology, Energy and Mines, Manitoba Geological Survey, Geoscientific Map MAP2008-1, scale 1:50 000 (plus notes and appendix).

Good, D., Mealin, C. and Walford, P. 2009: Geology of the Ore Fault Ni-Cu deposit, Bird River Sill complex, Manitoba; Exploration and Mining Geology, v. 18, p. 41–57.

Gorton, M.P. and Schandl, E.S. 2000: From continents to island arcs: a geochemical index of tectonic setting for arc-related and within-plate felsic to intermediate volcanic rocks; Canadian Mineralogist, v. 38, p. 1065–1073.

Hiebert, R. 2003: Composition and genesis of chromite in the Mayville intrusion, southeastern Manitoba; B.Sc. thesis, University of Manitoba, Winnipeg, Manitoba, 96 p.

Hoatson, D.H. 1998: Platinum-group element mineralisation in Australian Precambrian layered mafic-ultramafic intrusions; AGSO Journal of Australian Geology & Geophysics, v. 17, p. 139–151.

Hoffman, P.H. 1988: United plates of America, the birth of a craton: Early Proterozoic assembly and growth of Laurentia; Annual Review of Earth and Planetary Sciences, v. 16, p. 543–603.

Houlé, M.G., Gibson, H.L., Lesher, C.M., Davis, P.C., Cas, R.A.F., Beresford, S.W. and Arndt, N.T. 2008: Komatiitic sills and multigenerational peperite at Dundonald Beach, Abitibi greenstone belt, Ontario: volcanic architecture and nickel sulfide distribution; Economic Geology, v. 103, p. 1269–1284.

Hulbert, L. and Scoates, J. 2000: Digital map and database of magmatic Ni-Cu±PGE occurrences and mafic-ultramafic bodies in Manitoba; Manitoba Industry, Trade and Mines, Manitoba Geological Survey, Economic Geology Report ER2000-1, CD-ROM.

Keays, R.R. and Lightfoot, P.C. 2010: Crustal sulfur is required to form magmatic Ni-Cu sulfide deposits: evidence from chalcophile element signatures of Siberian and Deccan Trap basalts; Mineralium Deposita, v. 45, p. 241–257.

Kremer, P. 2010: Structural geology and geochronology of the Bernic Lake area in the Bird River greenstone belt, Manitoba: evidence for syn-deformational emplacement of the Bernic Lake pegmatite group; M.Sc. thesis, University of Waterloo, Waterloo, Ontario, 100 p.

Kremer, P.D. and Lin, S. 2006: Structural geology of the Bernic Lake area, Bird River greenstone belt, southeastern Manitoba (NTS 52L6): implications for rare element pegmatite emplacement; *in* Report of Activities 2006, Manitoba Science, Technology, Energy and Mines, Manitoba Geological Survey, p. 206–213.

Le Mée, L., Girardeau, J. and Monnier, C. 2004: Mantle segmentation along the Oman ophiolite fossil midocean ridge; Nature, v. 432, p. 167–172.

Lemkow, D.R., Sanborn-Barrie, M., Bailes, A.H., Percival, J.A., Rogers, N., Skulski, T., Anderson, S.D, McNicoll, V., Whalen, J.B., Tomlinson, K.Y., Parker, J.R., Hollings, P. and Young, M. 2006: GIS compilation of geology and tectonostratigraphic assemblages, western Uchi Subprovince, western Superior Province, Ontario and Manitoba; Geological Survey of Canada, Open File 5269, Manitoba Geological Survey, Open File OF2006-30, Ontario Geological Survey, Miscellaneous Release–Data 203, scale 1:250 000, CD-ROM.

Lightfoot, P.C., Naldrett, A.J., Gorbachev, N.S., Doherty, W. and Fedorenko, V.A. 1990: Geochemistry of the Siberian Trap of the Noril›sk area, USSR, with implications for the relative contributions of crust and mantle to flood basalt magmatism; Contributions to Mineralogy and Petrology, v. 104, p. 631–644.

Macek, J.J. 1985a: Cat Creek project (parts of 52L/1, 8); *in* Report of Activities 1985, Manitoba Energy and Mines, Mineral Resources Division, p. 122–129.

Macek, J.J. 1985b: Cat Creek; Manitoba Energy and Mines, Preliminary Map 1985C-1, scale 1:10 000.

Mackie, R.A. 2003: Emplacement history and PGE-enriched sulphide mineralization of the heterolithic breccia zone in the Mayville intrusion; B.Sc. thesis, University of Manitoba, Winnipeg, Manitoba, 135 p.

Manitoba Energy and Mines 1987: Pointe du Bois, NTS 52L; Manitoba Energy and Mines, Minerals Division, Bedrock Geology Compilation Map Series, NTS 52L, preliminary edition, scale 1:250 000.

McDonough, W.F. and Sun, S.-s. 1995: The composition of the Earth; Chemical Geology, v. 120, p. 223–253.

McGregor, C.R. 1986: Subsurface Precambrian geology of southeastern Manitoba south of 49 degrees 30 minutes; *in* Report of Field Activities 1986, Manitoba Energy and Mines, Minerals Division, p. 139–140.

Mealin, C.A. 2008: Geology, geochemistry and Cr-Ni-Cu-PGE mineralization of the Bird River sill: evidence for a multiple intrusion model; M.Sc. thesis, University of Waterloo, Waterloo, Ontario, 155 p.

Miyashiro, A. 1974: Volcanic-rock series in island arcs and active continental margins; American Journal of Science, v. 274, p. 321–355.

Murphy, L.A. and Theyer P. 2005: Geology, structure and mineralization of the Ore Fault property, Bird River greenstone belt, southeastern Manitoba (parts of NTS 52L5NE and 52L6NW); *in* Report of Activities 2005, Manitoba Industry, Economic Development and Mines, Manitoba Geological Survey, p. 156–160.

Mustang Minerals Corp. 2011: Annual report, 2010; Mustang Minerals Corp., 40 p.

Naldrett, A.J. 2004: Magmatic sulfide deposits; Springer, Berlin, 727 p.

Peck, D.C., Scoates, R.F.J., Theyer, P., Desharnais, G., Hulbert, L.J. and Huminicki, M.A.E. 2002: Stratiform and contact-type PGE-Cu-Ni mineralization in the Fox River Sill and the Bird River Belt, Manitoba; *in* The Geology, Geochemistry, Mineralogy and Mineral Beneficiation of Platinum-Group Elements, L.J. Cabri (ed.), Canadian Institute of Mining and Metallurgy, Special Volume 54, p. 367–387.

Peck, D.C., Theyer, P., Bailes, A.H. and Chornoby, J. 1999: Field and lithogeochemical investigations of mafic and ultramafic rocks and associated Cu-Ni-PGE mineralization in the Bird River greenstone belt (parts of NTS 52L); *in* Report of Activities, 1999, Manitoba Industry, Trade and Mines, Geological Services, p. 106–110.

Peck, D.C., Theyer, P., Hulbert, L., Xiong, J., Fedikow, M.A.F. and Cameron, H.D.M. 2000: Preliminary exploration database for platinum-group elements in Manitoba; Manitoba Industry, Trade and Mines, Manitoba Geological Survey, Open File OF2000-5, CD-ROM.

Percival, J.A. 2007: Geology and metallogeny of the Superior Province, Canada; *in* Mineral Deposits of Canada: A Synthesis of Major Deposit-Types, District Metallogeny, the Evolution of Geological Provinces, and Exploration Methods, W.D. Goodfellow (ed.), Geological Association of Canada, Mineral Deposits Division, Special Publication 5, p. 903–928.

Percival, J.A., McNicoll, V. and Bailes, A.H. 2006a: Strike-slip juxtaposition of ca. 2.72 Ga juvenile arc and >2.98 Ga continent margin sequences, and its implications for Archean terrane accretion, western Superior Province, Canada; Canadian Journal of Earth Sciences, v. 43, p. 895–927.

Percival, J.A., Sanborn-Barrie, M., Skulski, T., Stott, G.M., Helmstaedt, H. and White, D.J. 2006b: Tectonic evolution of the western Superior Province from NATMAP and LITHOPROBE studies; Canadian Journal of Earth Sciences, v. 43, p. 1085–1117.

Rollinson, H.R., Reid, C. and Windley, B. 2010: Chromitites from the Fiskenæsset anorthositic complex, West Greenland: clues to late Archaean mantle processes; *in* The Evolving Continents: Understanding Processes of Continental Growth, Kusky, T.M., Zhai, M.-G. and Xiao, W. (ed.), Geological Society of London, Special Publication 338, p. 197–212.

Ross, P.-S. and Bédard, J.H. 2009: Magmatic affinity of modern and ancient subalkaline volcanic rocks determined from trace-element discriminant diagrams; Canadian Journal of Earth Sciences, v. 46, p. 823–839.

Scoates, R.F.J. 1983: A preliminary stratigraphic examination of the ultramafic zone of the Bird River Sill, southeastern Manitoba; *in* Report of Field Activities, Manitoba Department of Energy and Mines, Mineral Resources Division, p. 70–83.

Scoates, R.F.J., Williamson, B.L., Eckstrand, O.R. and Duke, J.M. 1989: Stratigraphy of the Bird River Sill and its chromitiferous zone, and preliminary geochemistry of the chromitite layers and PGE-bearing units, Chrome property, Manitoba; *in* Investigations by the Geological Survey of Canada in Manitoba and Saskatchewan during the 1984–1989 Mineral Development Agreements, A.G. Galley (ed.), Geological Survey of Canada, Open File 2133, p. 69–82.

Springer, G.D. 1949: Geology of the Cat Lake–Winnipeg River area; Manitoba Mines Branch, Preliminary Report 48-7, 15 p.

Springer, G.D. 1950: Mineral deposits of the Cat Lake–Winnipeg River area; Manitoba Mines and Natural Resources, Mines Branch, Publication 49-7, 14 p.

Stevenson, R.K., Bernier, F., Courteau, G. and Achado, N. 2000: Nd isotopic studies of the buried Precambrian crust in southern Manitoba; *in* Western Superior Transect, 6th Annual Workshop, R.M. Harrap and H.H. Helmstaedt (ed.), LITHOPROBE Secretariat, University of British Colombia, Vancouver, British Columbia, LITHOPROBE Report 77, p. 116–118.

Stott, G.M., Corkery, M.T., Percival, J.A., Simard, M. and Goutier, J. 2010: A revised terrane subdivision of the Superior Province; Summary of Field Work and Other Activities 2010, Ontario Geological Survey, Open File Report 6260, p. 20-1–20-10.

Sun, S.-s. and McDonough, W.F. 1989: Chemical and isotopic systematics of oceanic basalts: implications for mantle composition and processes; *in* Magmatism in the Ocean Basins, A.D. Saunders and M.J. Norry (ed.), Geological Society of London, Special Publication 42, p. 313–345.

Syme, E.C. 1998: Ore-associated and barren rhyolites in the central Flin Flon belt: case study of the Flin Flon mine sequence; Manitoba Energy and Mines, Geological Services, Open File OF98-9, 26 p.

Syme, E.C., Lucas, S.B., Bailes, A.H. and Stern, R.A. 1999: Contrasting arc and MORB-like assemblages in the Paleoproterozoic Flin Flon Belt, Manitoba, and the role of intra-arc extension in localizing volcanic-hosted massive sulphide deposits; Canadian Journal of Earth Sciences, v. 36, p. 1767–1788.

Taylor, S.R. and McLennan S.M. 1985: The continental crust: its composition and evolution; Blackwell Scientific, Oxford, United Kingdom, 312 p.

Theyer, P. 1986: Platinum group elements in southeastern Manitoba; *in* Report of Field Activities 1986, Manitoba Energy and Mines, Geological Services Branch, p. 125–130.

Theyer, P. 2003: Platinum group element investigations in the Mayville igneous complex, southeastern Manitoba (NTS 52L12); *in* Report of Activities 2003, Manitoba Industry, Trade and Mines, Manitoba Geological Survey, p. 196–199.

Trueman, D.L. 1980: Stratigraphy, structure and metamorphic petrology of the Archean greenstone belt at Bird River, Manitoba; Ph.D. thesis, University of Manitoba, Winnipeg, Manitoba, 150 p.

Trueman, D.L. and Macek, J.J. 1971: Ultramafic project: geology of the Bird River Sill; Manitoba Department of Mines, Resources and Environmental Management, Mines Branch, Preliminary Map 1971-A1.

Veldhuyzen, H. 1995: Aluminium extraction from an Ontario calcic anorthosite by acid processes and resultant products—aluminium chemicals, coatings, fillers, absorbent and cement additive; Ontario Geological Survey, Open File Report 5919, 281 p.

Wang, X. 1993: U-Pb zircon geochronology study of the Bird River greenstone belt, southeastern Manitoba; M.Sc. thesis, University of Windsor, Windsor, Ontario, 96 p.

Yang, X.M. 2012: Bedrock geology of the Cat Creek area, Bird River greenstone belt, southeastern Manitoba (part of NTS 52L12); Manitoba Innovation, Energy and Mines, Manitoba Geological Survey, Preliminary Map PMAP2012-3, scale 1:12 500.

Yang, X.M., Gilbert, H.P., Corkery, M.T. and Houlé, M.G. 2011: The Mayville mafic–ultramafic intrusion in the Neoarchean Bird River greenstone belt, southeastern Manitoba (part of NTS 52L12): preliminary geochemical investigation and implication for PGE-Ni-Cu-(Cr) mineralization; *in* Report of Activities 2011, Manitoba Innovation, Energy and Mines, Manitoba Geological Survey, p. 127–142.

Yuan, F., Zhou, T., Zhang, D., Jowitt, S.M., Keays, R.R., Liu, S. and Fan, Y. 2012: Siderophile and chalcophile metal variations in basalts: implications for the sulphide saturation history and Ni-Cu-PGE mineralization potential of the Tarim continental flood basalt province, Xinjiang Province, China; Ore Review Geology, v. 45, p. 5–15.